Acceptor Behavior and E–H Bond Activation Processes of the Unsaturated Heterometallic Anion [MoReCp(μ-PCy$_2$)(CO)$_5$]$^-$ (Mo=Re)

M. Angeles Alvarez, M. Esther García, Daniel García-Vivó,* Estefanía Huergo, and Miguel A. Ruiz*

Departamento de Química Orgánica e Inorgánica / IUQOEM, Universidad de Oviedo, E-33071 Oviedo, Spain.

Supporting Information Placeholder

ABSTRACT: The ability of the title anion to act as an acceptor of simple donors and to participate in E–H bond activation processes (E = p-block element) was analyzed by examining its reactions with PPh_2H, HSPh and HCC(*p*-tol). The sodium salt of this anion (**1-Na**) reacted with PPh_2H to give the electron-precise derivative Na[MoReCp(μ-PCy_2)(CO)$_5$(PPh_2H)], with the added ligand *trans* to the PCy_2 group. The latter reacted with $(NH_4)PF_6$ to give the hydride-bridged derivative *mer*-[MoReCp(μ-H)(μ-PCy_2)(CO)$_5$(PPh_2H)], which was dehydrogenated photochemically to give first the known compound [MoReCp(μ-PCy_2)(μ-PPh_2)(CO)$_5$], and then the new complex [MoReCp(μ-O)(μ-PCy_2)(μ-PPh_2)(CO)$_3$], with a strongly asymmetric bridging oxide ligand (Mo–Re = 2.8640(6) Å). The reaction of **1-Na** with HSPh involved protonation and ligand addition to give the thiol complex [MoReCp(μ-H)(μ-PCy_2)(CO)$_5$(HSPh)], which underwent spontaneous dehydrogenation to give the thiolate derivative [MoReCp(μ-PCy_2)(μ-SPh)(CO)$_5$] (Mo–Re = 2.9702(8) Å), having a quite puckered central MoPReS ring. The latter rearranged photochemically to yield [MoReCp(μ-PCy_2)(μ-SPh)(1κ-CO)(CO)$_4$], which displays a Re(CO)$_4$ fragment and reverts thermally to the starting isomer; density functional theory calculations on these and related [MoReCp(μ-PCy_2)(μ-X)(CO)$_5$] complexes (X = PPh_2, Cl) revealed that the structure with the puckered central ring is strongly disfavored for bulky X groups. Compound **1-Na** reacted with (*p*-tolyl)acetylene to give complex Na[MoReCp(μ-PCy_2)(CO)$_5$\{η^2-HC_2(*p*-tol)\}], with an alkyne ligand η^2-bound to Re and positioned *cis* to the PCy_2 group. Protonation of the latter gave the alkenyl complex [MoReCp\{μ-κ^1:η^2-C(*p*-tol)CH_2\}(μ-PCy_2)(CO)$_5$], which rearranged spontaneously *via* alkenyl-carbonyl coupling and different 1,2-H shifts to give [MoReCp\{μ-η^2:$\kappa^2_{C,O}$-C(*p*-tol)CHC(O)H\}(μ-PCy_2)(CO)$_4$], with a formyl-alkenyl ligand *O*-bound to Re through its formyl fragment (Mo–Re = 2.970(1) Å).

INTRODUCTION

Mononuclear transition-metal carbonyl anions are classical reagents in organometallic synthesis. Thanks to their good nucleophilic properties, these species are very useful synthetic intermediates to make new bonds between transition-metal atoms and many other elements, not only H and C, but almost any other p- and d-block element, as revealed by extensive studies developed around these usually quite air-sensitive species.[1] The chemistry of binuclear carbonyl anions, however, has been comparatively much less studied, due to the reduced availability of suitable species of this type. Moreover, within the latter group, only a handful of complexes display intermetallic multiple bonds, and even fewer proved to be suitable for detailed studies of their reactivity, these being limited to the 32-electron complexes [Mn_2(CO)$_6$(μ-$Ph_2PCH_2PPh_2$)]$^{2-}$,[2] and [Fe_2(μ-PPh_2)(CO)$_6$]$^-$,[3] with M=M bonds, and to the 30-electron complexes [M_2Cp_2(μ-PR_2)(μ-CO)$_2$]$^-$ (M = Mo, R= Cy,[4] ^{t}Bu;[5] M = W, R = Cy),[6] with M≡M bonds. Extensive studies carried out on the latter dimolybdenum and ditungsten anions proved that the combined presence of negative charge and an intermetallic multiple bond confers a wide synthetic potential to these complexes, thus enabling the formation of a plethora of derivatives, both unsaturated and electron-precise ones, with many different functionalities, these including bridging hydride, alkyl, alkenyl and carbyne ligands, among others, sometimes with novel structures that cannot be achieved when using more conventional synthetic routes.[7] As a natural extension of this chemistry, we undertook a search for related unsaturated anions that would display intermetallic bonds between different transition metal elements, so as to add site selectivity and cooperative effects to the reactivity of the intermetallic multiple bond in these anionic species. Recently, we implemented efficient synthetic procedures for the phosphanide-stabilized unsaturated anion [MoReCp(μ-PCy_2)(CO)$_5$]$^-$ (**1**), which actually is the first binuclear carbonylate ever reported to display an heterometallic multiple bond.[8,9] As any other species bearing an intermetallic multiple bond, this complex is expected to exhibit ambiphilic (nucleophilic and electrophilic) behavior, which in this case can be further rationalized by inspection of the corresponding frontier orbitals. The most favorable position for addition of simple electrophiles to this MoRe anion (nucleophilic behavior) is the intermetallic region, and follows from interaction of the electrophile with the HOMO–2 orbital, which has Mo–Re bonding character.[8] The close HOMO–1 orbital is mainly located at the Mo atom, and it might serve to this purpose too, but incorporation of electrophiles at this position has not been observed so far, perhaps because this site is protected from

electrophilic attack by the Cp ring. On the other hand, the most favorable position for incorporation of simple donor molecules (electrophilic behavior of the anion) is indicated by the corresponding LUMO, which is mainly centered at the Re atom and exhibits partial π*(Mo–Re) character. Accordingly, the sodium salt of this anion (**1-Na**) readily added CO at the Re site to yield the electron-precise derivative [MoReCp(μ-PCy$_2$)(CO)$_6$]$^-$ (Scheme 1).[8] In this paper we further explore the electrophilic behavior of the unsaturated anion **1** by examining its reactions with some simple p-block element (E) donors having E–H bonds, such as the secondary phosphine PPh$_2$H, the thiol HSPh and the 1-alkyne HCC(*p*-tol). Through these reactions, we aimed to check the ability of this heterometallic anion to induce the activation of such bonds and related rearrangements, and to identify site selectivity and cooperative effects. As we will show below, the mentioned donor molecules readily add to anion **1** under mild conditions, but E–H bond activation only takes place in the neutral derivatives following from protonation of the resulting anionic intermediates.

Scheme 1. Carbonylation of Anion 1

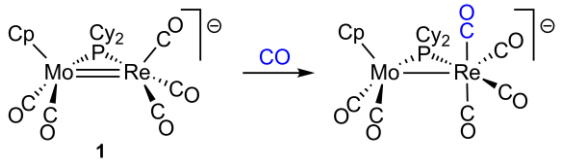

RESULTS AND DISCUSSION

Diphenylphosphine Derivatives of Anion 1. The unsaturated compound **1-Na** reacts rapidly with stoichiometric amounts of diphenylphosphine in tetrahydrofuran solution at room temperature to give the corresponding electron-precise derivative Na[MoReCp(μ-PCy$_2$)(CO)$_5$(PPh$_2$H)] (**2-Na**) as the single product (Scheme 2). Although we were not able to isolate this air-sensitive complex as a pure solid, the available spectroscopic data leave little doubt about the presence in this complex of a phosphine ligand with an intact P–H bond and coordinated at the Re atom *trans* to the phosphanide ligand (*vide infra*). This positioning is somewhat unexpected by considering the spatial orientation of the LUMO in **1**,[8] which rather would direct the incorporation of any generic ligand to a position *cis* to the phosphanide group. Perhaps, phosphine coordination on anion **1** takes place initially at the latter position, this being followed by a fast rearrangement to the final *trans* positioning, more favored on steric grounds (minimum repulsions between bulky PCy$_2$ and PPh$_2$H ligands). On the other hand, we note that attempts to force the cleavage of the phosphine P–H bond by refluxing tetrahydrofuran solutions of this salt led to no changes in the anion after 2 h. This is likely due to the saturated nature of this anion.

Compound **2-Na** is readily protonated at the intermetallic bond upon stirring with (NH$_4$)PF$_6$, to give the corresponding hydride-bridged derivative *mer*-[MoReCp(μ-H)(μ-PCy$_2$)(CO)$_5$(PPh$_2$H)] (**3**) in high yield, a product which can be isolated in a conventional way. Attempts to induce the cleavage of the phosphine P–H bond in this neutral product by refluxing its toluene solutions led to no significant change after 1 h. However, irradiation of tetrahydrofuran solutions of **3** at room temperature induced a fast dehydrogenation that led to the known bis(phosphanide) complex [MoReCp(μ-PCy$_2$)(μ-PPh$_2$)(CO)$_5$] in a selective way (Scheme 2). This complex has been recently identified by us as the product following from the photolysis of *fac*-[MoReCp(μ-H)(μ-PCy$_2$)(CO)$_5$(PPh$_2$H)], an isomer of **3** bearing a PPh$_2$H ligand positioned *cis* to the phosphanide group.[9] In the photolysis of **3**, however, we noticed that the use of prolonged irradiation times led to the progressive decomposition of the initial bis(phosphanide) complex (δ_P 189.9 and 153.0 ppm) to give a green product displaying much more shielded resonances (δ_P 80.3 and 44.0 ppm). We afterwards found that this product can be actually prepared in better yield (ca. 87%) upon refluxing toluene solutions of [MoReCp(μ-PCy$_2$)(μ-PPh$_2$)(CO)$_5$] for ca. 2 h, and eventually we have identified it as the oxide-bridged complex [MoReCp(μ-O)(μ-PCy$_2$)(μ-PPh$_2$)(CO)$_3$] (**4**). Although the actual source of oxygen in the formation of this air-sensitive product has not been clearly identified, this oxide complex most likely follows from the reaction of the unsaturated species following decarbonylation with trace amounts of oxygen present in the reaction medium.

Scheme 2. Diphenylphosphine Derivatives of Anion 1

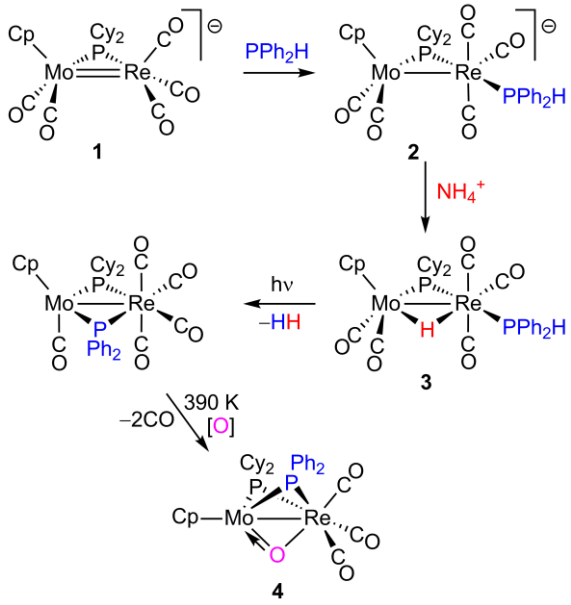

Structural Characterization of Diphenylphosphine Complexes 2 and 3. The IR spectrum of **2-Na** displays four C–O stretches with frequencies not very different from those of the parent anion (Table 1). However, the most energetic band, essentially corresponding to the symmetric stretch of the Re(CO)$_3$ oscillator, displays a very weak intensity, thus denoting a meridional distribution of carbonyls at this fragment.[10] On the other hand, the phosphine ligand in this anion gives rise to a ^{31}P NMR resonance displaying a large coupling of 67 Hz to the phosphanide ligand, which is indicative of a transoid positioning of these P-donor atoms in a pseudo-octahedral environment.[11] For comparison, the PP coupling in the complex *fac*-[MoReCp(μ-H)(μ-PCy$_2$)(CO)$_5$(PPh$_2$H)] mentioned above (with P ligands at angles close to 90º) was much lower (22 Hz).[9] Finally, the retention of the P–H bond in the newly incorporated P-donor ligand in **2-Na** is denoted by the large splitting of the phosphine resonance (δ_P 6.6 ppm) upon ^{1}H coupling ($^1J_{HP}$ = 347 Hz).

The IR C–O stretches of **3** (Table 1) are comparable to those of its anionic precursor **2-Na**, but displaced some 60-100 cm^{-1} towards higher frequencies, as expected upon protonation

of a binuclear anion at the intermetallic bond with retention of the overall geometry. The meridional arrangement of the carbonyls at the octahedral Re fragment is again indicated by the weak intensity of the band at the highest frequency (2036 cm^{-1}), while the large coupling of 65 Hz between the P atoms indicates the transoid positioning of the corresponding ligands, as found in its anionic precursor. In agreement with this, the resonance of the hydride ligand of **3** (δ_H −13.07 ppm), which is positioned *cis* to both P atoms of the complex, displays low and comparable couplings to these atoms (16 and 18 Hz). The retention of the P–H bond in the phosphine ligand of **3** is denoted by the large splitting (by 358 Hz) of the –22.0 ppm ^{31}P NMR resonance of the complex upon ^{1}H coupling, and by the direct observation of the corresponding resonance in the ^{1}H NMR spectrum (δ_H 7.44 ppm, see the Experimental Section).

Table 1. Selected IR and NMR Data for New Compounds

Compound	ν(CO)[a]	δ_P(J_{PP})[b]
Na[MoReCp(μ-PCy_2)$(CO)_5$] (**1-Na**)[c]	1973 (s), 1875 (vs), 1860 (vs), 1803 (w)[d]	129.2[d]
Na[MoReCp(μ-PCy_2)$(CO)_5(PPh_2H)$] (**2-Na**)[d]	1978 (w), 1888 (vs), 1855 (s), 1780 (w, br), 1715 (w)[d]	161.4 (67) 6.6 (67)[d,e]
mer-[MoReCp(μ-H)(μ-PCy_2)$(CO)_5(PPh_2H)$] (**3**)	2036 (w), 1948 (vs), 1936 (m), 1920 (m), 1877 (m) [f]	146.0 (65) –22.0 (65)[g]
[MoReCp(μ-O)(μ-PCy_2)(μ-PPh_2)$(CO)_3$] (**4**)	2009 (vs), 1925 (m), 1898 (m)	80.3 (21) 44.0 (21)
[MoReCp(μ-H)(μ-PCy_2)$(CO)_5$(HSPh)] (**5**)	1990 (s), 1924 (vs), 1895 (s), 1864 (s), 1848 (m, sh), 1830 (w, sh)[d]	129.3 (*anti*) 130.1 (*syn*)[h]
[MoReCp(μ-PCy_2)(μ-SPh)$(CO)_5$] (**6**)	2012 (vs), 1980 (m), 1924 (m), 1899 (m), 1884 (m, sh)	52.6
[MoReCp(μ-PCy_2)(μ-SPh)(1κ-CO)$(CO)_4$] (**7**)	2091(w), 2004 (s), 1993 (vs), 1963 (s), 1818 (w)[f]	204.6[i]
Na[MoReCp(μ-PCy_2)$(CO)_5${η^2-HC_2(*p*-tol)}] (**8-Na**)	1978 (s), 1903 (m), 1868 (vs), 1854 (m, sh), 1809 (w)[d]	202.6[d]
[MoReCp{μ-κ^1:η^2-C(*p*-tol)CH_2}(μ-PCy_2)$(CO)_5$] (**9**)	2003 (vs), 1933 (s), 1904 (s, sh), 1894 (vs), 1875 (m, sh)	211.4[j]
syn-[MoReCp{μ-η^2:$\kappa^2_{C,O}$-C(*p*-tol)CHC(O)H}(μ-PCy_2)$(CO)_4$] (***syn*-10**)	2020 (vs), 1952 (m), 1892 (s)	229.4
anti-[MoReCp{μ-η^2:$\kappa^2_{C,O}$-C(*p*-tol)CHC(O)H}(μ-PCy_2)$(CO)_4$] (***anti*-10**)	2020 (vs), 1950 (s), 1890 (m)	245.4

[a] Recorded in dichloromethane solution, ν in cm^{-1}. [b] Recorded in CD_2Cl_2 solutions at 295 K and 121.50 MHz, with chemical shifts (δ) in ppm relative to external 85% aqueous H_3PO_4, and ^{31}P-^{31}P couplings (J_{PP}) in Hertz [c] Data taken from ref. 8. [d] In tetrahydrofuran solution. [e] The resonance at 6.6 ppm displayed a P–H coupling of 347 Hz in the corresponding ^{31}P NMR spectrum. [f] In petroleum ether. [g] The resonance at –22.0 ppm displayed a P–H coupling of 358 Hz in the corresponding ^{31}P NMR spectrum. [h] In tetrahydrofuran-d_8 solution; the complex is obtained as a 3:2 mixture *anti* and *syn* isomers (see text). [i] In tetrahydrofuran-d_8 solution at 233 K. [j] Recorded at 253 K.

Structure of the Oxide Complex 4. The molecule of **4** in the crystal (Figure 1 and Table 2) is built from MoCp and pyramidal $Re(CO)_3$ fragments connected by an oxide and two phosphanide (PCy_2 and PPh_2) ligands, so as to render pseudo-octahedral environments around both metal atoms (if considering the Cp ring as equivalent to three coordination positions). The coordination of the bridging groups is strongly asymmetric, with distances to the Mo atom significantly shorter than those to Re, likely to balance the lower electron count of the Mo fragment (11 vs. 13 electrons). These differences are even more significant after considering that the covalent radius for Mo is some 0.03 Å *large*r than the one for Re.[12] Thus, the Mo–P distances of ca. 2.38 Å for the phosphanide ligands are some 0.13 Å shorter than the corresponding Re–P separations (ca. 2.51 Å), while differences for the oxide ligand are much more pronounced (1.800(5) *vs.* 2.218(5) Å). Actually, the very short Mo–O distance in **4** approaches the figures of ca. 1.70 Å typically found for related cyclopentadienyl complexes bearing terminal M–O bonds (M = Mo, W),[13,14] thus indicating considerable multiplicity in that bond. According to this, the oxide ligand in **4** should be better considered as a four-electron donor formally providing the metal centers with 3 (Mo) and 1 (Re) electrons respectively, in other words, with a π bonding interaction located at the O–Mo connection. A similar asymmetric coordination of a bridging oxide ligand has been previously proposed by us for the oxide nitride complexes [Mo_2MCp_2Cp'(μ-N)(μ-O)(μ-PR_2)$(CO)_3$] (R = Ph, Cy; M = Mn, Re),[15] and substantiated by density functional theory (DFT) calculations on the PPh_2-bridged Mo_2Mn complex. In the case of **4**, the strong binding of the oxide ligand to the Mo atom is also reflected in a significant lengthening of some 0.15 Å in the Mo–C distances of cyclopentadienyl carbons positioned *trans* to it (C5 and C6). Such a strong *trans* influence is a characteristic feature of cyclopentadienyl complexes bearing terminal oxide ligands.[13]

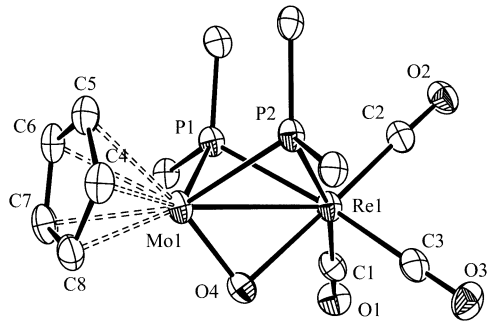

Figure 1. ORTEP drawing (30% probability) of **4**, with Cy and Ph groups (except their C1 atoms), and H atoms omitted.

Table 2. Selected Bond Lengths (Å) and Angles (°) for 4.

Mo1–Re1	2.8640(6)	Mo1–P1–Re1	71.68(4)
Mo1–P1	2.377(2)	Mo1–P2–Re1	71.48(4)
Re1–P1	2.511(2)	Mo1–O4–Re1	90.3(2)
Mo1–P2	2.393(2)	P1–Mo1–P2	83.76(6)
Re1–P2	2.508(2)	P1–Mo1–O4	92.7(2)
Mo1–O4	1.800(5)	P2–Mo1–O4	90.9(2)
Re1–O4	2.218(5)	P1–Re1–P2	78.76(5)
Re1–C1	1.953(7)	P1–Re1–C1	93.3(2)
Re1–C2	1.918(7)	P1–Re1–C2	99.0(2)
Re1–C3	1.956(7)	P1–Re1–C3	170.0(2)
Mo1–C5	2.412(7)	P2–Re1–C1	166.4(2)
Mo1–C6	2.427(7)	P2–Re1–C2	99.5(2)
Mo1–C8	2.261(7)	P2–Re1–C3	94.5(2)

Chart 1

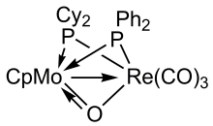

The localized π-bonding of the oxide ligand in **4**, taken along with the asymmetric coordination of the phosphanide ligands, renders a reasonably balanced electron count on the metal atoms of this 34-electron complex, for which an intermetallic single bond should be therefore proposed according to the 18-electron formalism (a dative bond, in the extreme representation depicted in Chart 1). The intermetallic separation of 2.8640(6) Å in **4**, while significantly shorter than the reference value of 3.05 Å for a Mo–Re bond,[12] still is consistent with a single-bond formulation after allowing for the shortening effect derived from the presence of three bridging ligands connecting the metal atoms, a structural effect well established for thiolate-bridged cyclopentadienyl dimolybdenum complexes.[16] Unfortunately, no oxide-bridged MoRe binuclear complexes appear to have been structurally characterized so far, to be used for comparative purposes. However, a few WRe_2 organometallic clusters have been reported with oxide ligands bridging over WRe edges.[17] Even if the coordination spheres in these clusters are not strictly comparable to those in **4**, it is interesting to note that all of them also display strongly asymmetric oxide ligands (W–O = 1.77-1.80 Å; Re–O = 2.14-2.29 Å) bridging over short W–Re edges (2.79-2.87 Å), as found in **4**.

Spectroscopic data in solution for **4** are consistent with the structure found in the crystal and deserve only a few comments. The retention of the pseudo-octahedral geometry around the rhenium atom is indicated by the IR spectrum, which displays three C–O stretches with the characteristic intensities of pyramidal $M(CO)_3$ oscillators,[10] while the low coupling of 21 Hz between the P atoms of the phosphanide ligands (cf. 67 Hz in **3**) is indicative of their cisoid positioning (P–M–P ca. 81° in the crystal). In the same line, the carbonyl ^{13}C NMR resonances display the expected pattern for the couplings to the P atoms,[11] with two of them displaying one large (ca. 33 Hz, *trans* to P) and one small coupling (ca. 7 Hz, *cis* to P), while the third one displays a small coupling of 5 Hz to both P atoms.

Thiophenol Derivatives of Anion 1. Compound **1-Na** reacts rapidly with two equivalent of thiophenol, in tetrahydrofuran solution at room temperature, to give quantitatively the neutral hydride-bridged thiol complex [MoReCp(μ-H)(μ-PCy_2)$(CO)_5$(HSPh)] (**5**) (Scheme 3), which is formed as a ca. 3:2 mixture of two isomers. These isomers presumably differ in the relative positioning (*syn* or *anti*) of the Cp and thiol ligands with respect to the average plane of the central Mo(μ-P)(μ-H)Re ring of the molecule (Chart 2), with the major isomer likely displaying the *anti* conformation, more favored on steric grounds. In any case, we note that the formation of the thiol complex **5** parallels the reaction of **1-Na** with the ammonium cation, which selectively yields the related hydride-bridged ammonia complex [MoReCp(μ-H)(μ-PCy_2)$(CO)_5(NH_3)$].[8] Since the Brönsted acidity of thiophenol (pk_a ca. 6) is higher than that of the ammonium cation, it is reasonable to assume that the thiol reaction is initiated by protonation of the anion at the intermetallic bond. This would give the unstable unsaturated hydride [MoReCp(μ-H)(μ-PCy_2)$(CO)_5$] (an intermediate not detected) which rapidly would evolve by adding a second thiol molecule, to eventually yield the electron-precise derivative **5**.

Scheme 3. Thiophenol Derivatives of Anion 1

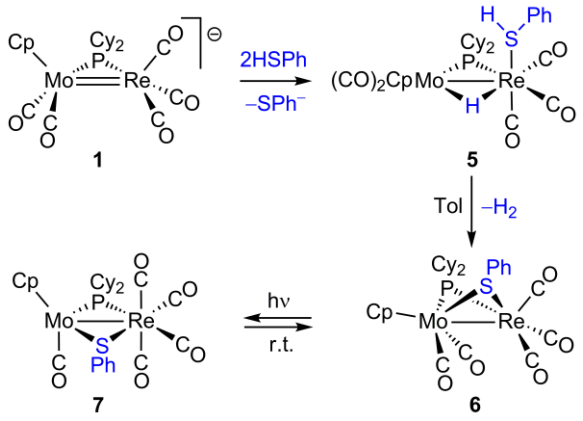

Chart 2

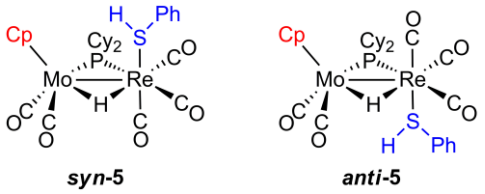

***syn*-5** ***anti*-5**

Although compound **5** is stable for a few hours in tetrahydrofuran solution at room temperature, all attempts to isolate this complex as a pure solid were unsuccessful, as dehydrogenation takes place by just removing the solvent under vacuum or upon attempted chromatography, all of this eventually yielding the stable thiolate-bridged derivative [MoReCp(μ-PCy_2)(μ-SPh)$(CO)_5$] (**6**), a product which can be isolated in good yield. Despite this, the available spectroscopic data for both isomers of **5** (Table 1 and Experimental Section) are very similar to each other and to those recently reported by us for related species of type *fac*-[MoReCp(μ-H)(μ-PCy_2)$(CO)_5$L] (L = NH_3, NCMe, PPh_2H),[8,9] thus leaving no doubt about the spatial positioning of the hydride and thiol ligands in these isomers. This is particularly so in the case of the P and hydride chemical shifts and couplings (δ_P ca. 130 ppm, δ_H ca. −11 ppm, J_{PH} ca. 21 Hz for both isomers of **5**, to be compared with δ_P = 135.1, δ_H = −10.56, J_{PH} = 20 for the ammonia complex), while the C–O stretching bands are some 10 cm^{-1} lower than those of the mentioned NH_3 complex, thus suggesting a stronger binding of the HSPh ligand in **5**. The ^1H NMR resonances for the S–H group in the isomers of **5** were located at 0.10 and 0.04 ppm, not far from the values reported for different chromium complexes of type [Cr$(CO)_4$L(HSR)] (L = CO, PEt_3), in the range 2.80-0.77 ppm.[18]

The room temperature dehydrogenation of **5** is surprising since we have recently prepared an isomer of it, [MoReCp(H)(μ-SPh)($PHCy_2$)$(CO)_5$], which does not undergo dehydrogenation in toluene solution at 333 K.[9] The latter isomer bears terminal H and $PHCy_2$ ligands bound to the Re atom, while **5** displays bridging H and terminal SHPh ligands. This structural difference, however, does not seem to justify their distinct behavior concerning dehydrogenation, which might instead follow from the higher polarity of the S–H bond when compared to the P–H bond.

Structure of the Thiolate Complex 6. The structure of **6** in the crystal (Figure 2 and Table 3) is built from MoCp$(CO)_2$ and pyramidal Re$(CO)_3$ fragments bridged by PCy_2 and SPh ligands, with the latter defining a central MoPReS ring even more puckered than the corresponding MoPReP ring in **4** (P–Mo–Re–S ca. 97° vs. P–Mo–Re–P ca. 107°). This defines a four-legged piano stool coordination environment around Mo, while the environment around Re might be described as square pyramidal, if we ignore the intermetallic interaction (distorted octahedral, if we take it into account). The latter should be described as a metal-metal single bond according to the 18-electron formalism, which is in agreement with the short intermetallic distance of 2.9702(8) Å. In all, the structure of **6** is comparable to that of the isoelectronic carboxylate-bridged complex [MoReCp{μ-O_2C(*p*-tol)}(μ-PCy_2)$(CO)_5$], which also displays a relatively short distance of 3.0332(2) Å.[9] It is interesting to note the structural differences between these two molecules and the isoelectronic bis(phosphanide) complex [MoReCp(μ-PCy_2)(μ-PPh_2)$(CO)_5$], which instead is built from MoCp(CO) and Re$(CO)_4$ fragments and displays an almost planar MoPReP central ring,[9] a matter to be discussed below.

To balance the different electron count of the MoCp$(CO)_2$ and Re$(CO)_3$ fragments in **6** (15 and 13 electrons, respectively), the P and S atoms should bridge asymmetrically the metal atoms, with formal contributions in both cases of 1 and 2 electrons to the Mo and Re atoms, respectively (Chart 3). This is in agreement with the observation of a Re–P distance which is 0.1 Å shorter than the corresponding Mo–P separation, but differences in the M–S lengths are somewhat lower (ca. 0.07 Å). Although no related MoRe complexes appear to have been structurally characterized so far (so direct comparisons are not possible), we note that in different MoMn complexes of type [MoMnCp(μ-SR)(μ-SR')$(CO)_5$] related to **6**,[19] relatively long Mo–S lengths (ca. 2.45-2.49 Å) were observed in all cases (cf. 2.529(2) Å in **6**), this pointing to a similarly asymmetric coordination of the bridging ligands in this sort of structures. For comparison, the Mo–S distances in the symmetrically-bridged cation [Mo_2Cp_2(μ-CPh)(μ-PCy_2)(μ-SPh)]$^+$ are ca. 2.42 Å.[20]

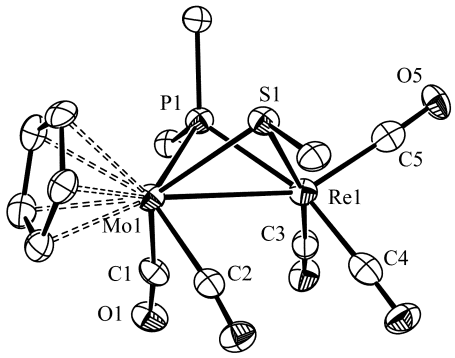

Figure 2. ORTEP drawing (30% probability) of **6**, with Cy and Ph groups (except their C^1 atoms), and H atoms omitted.

Table 3. Selected Bond Lengths (Å) and Angles (°) for 6.

Mo1–Re1	2.9702(8)	Mo1–P1–Re1	73.94(7)
Mo1–P1	2.519(2)	Mo1–S1–Re1	73.05(5)
Re1–P1	2.418(2)	P1–Mo1–S1	71.95(7)
Mo1–S1	2.529(2)	P1–Mo1–C1	80.5(3)
Re1–S1	2.461(2)	P1–Mo1–C2	125.2(3)
Mo1–C1	1.97(1)	C1–Mo1–C2	79.5(3)
Mo1–C2	2.02(1)	P1–Re1–C3	93.2(3)
Re1–C3	1.92(1)	P1–Re1–C4	162.3(3)
Re1–C4	1.94(1)	P1–Re1–C5	106.0(3)
Re1–C5	1.93(1)	C3–Re1–C4	89.6(4)

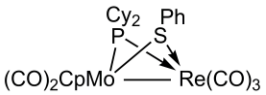

Chart 3

Spectroscopic data in solution for compound **6** are consistent with the geometry found in the crystal. Its IR spectrum

displays five C–O stretches, with the three most energetic ones (mainly derived from the Re fragment) displaying the pattern characteristic of pyramidal $M(CO)_3$ oscillators,[10] while the carbonyl ^{13}C NMR resonances display the expected P–C couplings, with values for carbonyls *trans* to the P ligand being larger than those of carbonyls *cis* to it at the Re fragment, while the opposite holds for the Mo fragment.[11,21] Surprisingly, the PCy_2 ligand gives rise to a rather shielded ^{31}P NMR resonance (δ_P 53.0 ppm), still below the chemical shift of the oxide complex **4** (δ_P 80.3 ppm). This spectral feature might be related to the puckering of the central MoPReX ring in these molecules (X = P, S), because isoelectronic complexes displaying flatter MoPReX rings seem to display more deshielded ^{31}P resonances for their PCy_2 ligands (129-245 ppm for all other compounds in this work, Table 1).

Structural Preferences in [MoReCp(μ-PCy_2)(μ-X)$(CO)_5$] Complexes. Isomerization of Compound 6. As noted above, the structure of the thiolate complex **6** (from now on denoted as type **A**) is dramatically different from that of the isoelectronic bis(phosphanide) complex [MoReCp(μ-PCy_2)(μ-PPh_2)$(CO)_5$] (denoted as type **B**), which instead is built from MoCp(CO) and $Re(CO)_4$ fragments, displays a nearly planar MoPReP central ring (P–Mo–Re–P ca. 164º), and a longer intermetallic length of 3.0970(5) Å.[9] To find out whether this difference is of thermodynamic origin or follows instead from the different synthetic routes (thermal vs. photochemical) used to prepare each of these compounds, we carried out DFT calculations on both types of structures for [MoReCp(μ-PCy_2)(μ-X)$(CO)_5$] complexes having different X ligands (denoted as **A-X** and **B-X**, with X = PPh_2, SPh, Cl; see the SI).

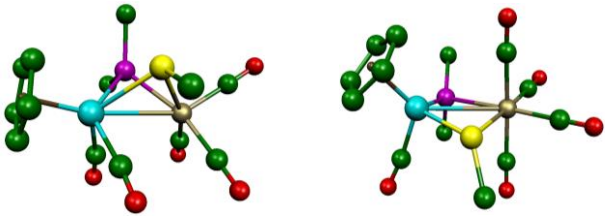

Figure 3. DFT-optimized structures of isomers **A-SPh** (left) and **B-SPh** (right) (compounds **6** and **7**, respectively), with Cy and Ph groups (except their C^1 atoms), and H atoms omitted.

Table 4. Selected DFT-computed Bond Lengths (Å) and Angles (º) for [MoReCp(μ-PCy_2)(μ-X)$(CO)_5$] Complexes.

Isomer	Mo–Re	ϕ^a	Δd(P)^b	Δd(X)^c	ΔG^d
A-PPh_2	3.155	107.2	0.163	0.153	+58
A-SPh	3.057	96.2	0.129	0.074	+4
A-Cl	3.025	98.4	0.125	0.031	0
B-PPh_2	3.215	156.7	–0.233	–0.389	0
B-SPh	3.191	165.1	–0.301	–0.156	0
B-Cl	3.215	156.9	–0.351	–0.043	+15

[a] P–Mo–Re–X dihedral angle. [b] d(Mo–P)–d(Re–P) for the PCy_2 ligand. [c] d(Mo–X)–d(Re–X) for the X ligand (X = PPh_2, SPh, Cl). [d] Gibbs free energy in the gas phase at 298 K (in kJ/mol) relative to the most stable isomer in each case.

First we note that the optimized structures for **A-SPh** (compound **6**) and **B-PPh_2** (see Figure 3 and the SI) are in good agreement with the corresponding structures determined crystallographically, although the computed distances involving the metal atoms are slightly overestimated, as commonly found in this sort of calculations.[22] Apart from this, the key structural differences in these two types of structures are well reproduced for all X ligands (Figure 3 and Table 4): (a) a strong puckering of the central MoPReX ring in isomers **A** (ca. 100º vs. 160º); (b) a distinct asymmetry in both PCy_2 and X bridges (larger in the former), which are closer to Re in isomers **A**, but closer to Mo in isomers **B**, to better balance the different electron counts of the corresponding metal fragments, and (c) a shorter intermetallic length (0.06-0.19 Å) for isomers of type **A**.

The computed Gibbs free energy values for this family of complexes reveal that the relative thermodynamic stability of isomers **A** and **B** depends strongly on the bridging ligands X, and seems particularly dependent on their steric requirements. Thus, the structure **A** is strongly disfavored (by 58 kJ/mol) for the bulkier PPh_2 group, obviously because of the severe steric repulsions between the Cy and Ph groups of the phosphanide ligands, forced into close positions by the puckered MoPReP central ring. At the other extreme, the structure **A** is significantly favored (by 15 kJ/mol) for the chloride-bridged complex. In that case, the absence of steric constraints allows for a closer approach of the metal fragments (Mo–Re = 3.025 Å), which enables a stronger intermetallic interaction (cf. 3.155 Å when X = PPh_2). Besides this, the higher electronegativity of Cl might be another factor working in the same direction, since we have recently shown that the intermetallic lengths in dimolybdenum complexes of the type [Mo_2Cp_2(μ-PR_2)(μ-X)$(CO)_2$] are shorter for X groups having more electronegative donor atoms.[5] The steric situation in the SPh-bridged compound is clearly intermediate, since the thiolate ligand in isomer **A** (compound **6**) can orientate its Ph ring away from the PCy_2 ligand, thus notably reducing the repulsive interactions between the bridging groups, evident in the PPh_2 complex. As a result, isomer **A** is less de-stabilized, and it is actually computed to have a Gibbs free energy similar to that of isomer **B** (4 kJ/mol above it in the gas phase, but just 0.2 kJ/mol in toluene solution).

The close thermodynamic stability computed for isomers **A** and **B** when X = SPh suggested that an isomerization of compound **6** might be possible. We first checked the thermal stability of this complex, and found that refluxing a toluene solution of **6** for 2 h induced no significant change in the molecule. In contrast, we found that irradiation of toluene solutions of **6** with visible-UV light causes its partial isomerization into the corresponding isomer of type **B**, formulated as [MoReCp(μ-PCy_2)(μ-SPh)(1κ-CO)$(CO)_4$] (**7**) (Scheme 3). However, this transformation cannot be completed, but just a ca. 3:2 mixture of **7** and **6** is obtained in toluene solution at room temperature. Moreover, we could not isolate pure samples of **7** because this complex decays thermally back to isomer **6** (which obviously is more stable), the transformation being complete in ca. 1 h at room temperature in toluene solution, as revealed by NMR monitoring experiments. Attempted separation of these mixtures through low-temperature chromatography on alumina or Florisil also failed, as rapid transformation of **7** into **6** was induced by these solid supports. Yet, the spectroscopic data obtained for **7** from the above mixtures (Table 1 and Experimental Section) are comparable to those of the bis(phosphanide) complex [MoReCp(μ-PCy_2)(μ-PPh_2)$(CO)_5$], and clearly reveal a structure of type **B** for this product. Par-

ticularly informative is the presence in the IR spectrum of a high frequency, medium intensity C–O stretch at 2091 cm^{-1}, which is indicative of the presence of a $Re(CO)_4$ fragment (cf. 2020 cm^{-1} for the $Re(CO)_3$ fragment of **6** in the same solvent), and a low-frequency band at 1818 cm^{-1} corresponding to the Mo(CO) oscillator, all of it in excellent agreement with the DFT computed C–O stretches for **B–SPh** (see the SI). Moreover, the ^{31}P nucleus of the PCy_2 ligand is strongly deshielded (δ_P 204.6 ppm) when compared to isomer **6**, and its chemical shift is comparable to the one measured for the mentioned bis(phosphanide) complex (δ_P 189.9 ppm).[9] This reinforces our view that the relatively large ^{31}P shielding observed for compounds **4** and **6** is related to the strong puckering of the central MoPReX ring in these molecules.

1-Alkyne Derivatives of Anion 1. Compound **1-Na** reacts with an excess of (*p*-tolyl)acetylene, in tetrahydrofuran solution at room temperature, to give selectively the alkyne complex $Na[MoReCp(\mu\text{-}PCy_2)(CO)_5\{\eta^2\text{-}HC_2(p\text{-}tol)\}]$ (**8-Na**) (Scheme 4). Although we were not able to isolate this air-sensitive species as a pure solid, the available spectroscopic data support the presence in this complex of an alkyne ligand η^2-bound to Re and positioned *cis* to the PCy_2 ligand, now in agreement with the spatial orientation of the LUMO in **1**.[8]

Scheme 4. 1-Alkyne Derivatives of Anion 1

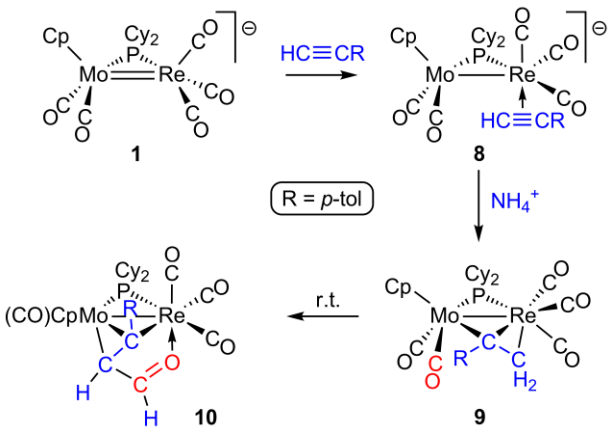

Upon reaction with $(NH_4)PF_6$, compound **8-Na** is immediately transformed into the neutral derivative $[MoReCp\{\mu\text{-}\kappa^1\text{:}\eta^2\text{-}C(p\text{-}tol)CH_2\}(\mu\text{-}PCy_2)(CO)_5]$ (**9**), which displays an α-substituted alkenyl ligand σ-bound to Mo and π bound to Re, according to the spectroscopic data and DFT calculations discussed below. Compound **9** is likely formed through protonation at the more accessible terminal carbon of the alkyne, but protonation at the intermetallic bond followed by fast insertion of the alkyne into the resulting Mo–H–Re bond cannot be excluded, since the latter is a typical reaction of hydride-bridged complexes with alkynes.[23] Unfortunately, we have not been able to isolate **9** as a pure solid either, since it rearranges progressively at room temperature to give the formyl-alkenyl derivative $[MoReCp\{\mu\text{-}\eta^2\text{:}\kappa^2_{C,O}\text{-}C(p\text{-}tol)CHC(O)H\}(\mu\text{-}PCy_2)(CO)_4]$ (**10**), along with a small amount of the known hydride $[MoReCp(\mu\text{-}H)(\mu\text{-}PCy_2)(CO)_6]$.[24] Compound **10** bears a *C,C*:*C,O*-bound hydrocarbyl ligand derived from alkenyl-carbonyl coupling in **9** along with a H-shift, and is obtained as a ca. 3:1 mixture of two isomers differing in the relative positioning (*syn* or *anti*) of the Mo-bound carbonyl and the Re-bound oxygen atom, relative to the average MoPReC plane defined by the central ring of the molecule (Chart 4). Fortunately, these isomers could be separated from each other through chromatography, and we were able to determine the structure of the minor isomer ***anti*-10** through a diffraction study.

Chart 4

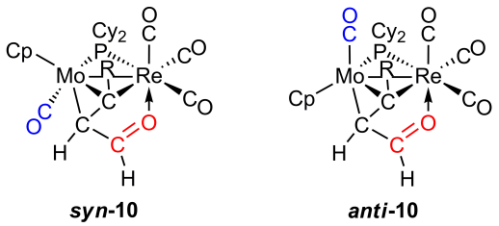

Structural Characterization of Compounds 8 and 9. The IR spectrum of **8-Na** (Table 1) displays C–O stretches of frequency comparable to those of **1-Na**, and the high intensity of the most energetic band at 1978 cm^{-1} denotes the presence of a pyramidal $Re(CO)_3$ fragment in the anion, as opposed to the situation in **2-Na**. This implies a coordination of the added alkyne *cis* to the P atom and nearly perpendicular to the central MoPRe ring of the anion, most likely in a disposition *anti* to the Mo-bound Cp ligand, to minimize steric repulsions (Scheme 4). The Re-bound alkyne gives rise to a ^1H NMR resonance at 5.99 ppm, and to ^{13}C resonances at 126.0 (internal) and 76.7 (CH) ppm. These data are consistent with a η^2-coordination of the alkyne (cf. δ_H ca. 5 ppm; δ_C ca. 90 and 70 (CH) ppm for $[ReCp^*(CO)_2(\eta^2\text{-}HCCR)]$ complexes),[25] although the chemical shift of the internal carbon is somewhat higher than expected. The latter might be related to the spatial proximity of other ligands in the anion; indeed, the variable-temperature ^1H and $^{13}C\{^1H\}$ NMR spectra of **8-Na** reveal slow rotation of the *p*-tol ring on the NMR timescale (see the Experimental Section), which obviously is indicative of severe steric congestion in the anion. We finally note that the ^{31}P chemical shift of the phosphanide ligand (δ_P 203.7 ppm) also is somewhat higher than expected (ca. 162 ppm for the isoelectronic anions **2** and $[MoReCp(\mu\text{-}PCy_2)(CO)_6]^-$), with no obvious reason for it. This spectroscopic feature, however, is also present in the neutral hydrocarbyl-bridged derivatives of anion **8** discussed below (compounds **9** and **10**).

The NMR spectra of **9** suggests the formation of a bridging σ:π-bound alkenyl ligand upon protonation of anion **8**, since two ^1H resonances are observed at 6.35 and 3.16 ppm with no resolvable mutual coupling, which is a common feature of geminal CH_2 groups, while the corresponding ^{13}C resonances are located at 184.5 (μ-C) and 75.3 (CH_2) ppm. These spectroscopic features are comparable to those of the related homonuclear complexes $[M_2Cp_2\{\mu\text{-}\kappa^1\text{:}\eta^2\text{-}C(p\text{-}tol)CH_2\}(\mu\text{-}PCy_2)(CO)_2]$ (M = Mo, W),[23] and to those of the recently reported heterometallic complex $[MoReCp(\mu\text{-}\kappa^1\text{:}\eta^2\text{-}CRCHR)(\mu\text{-}PCy_2)(CO)_5]$ (R = CO_2Me).[9] The latter displays ^{13}C NMR alkenyl resonances at 148.0 and 46.9 ppm, but bears its alkenyl ligand σ-bound to a $Re(CO)_4$ fragment and π-bound to a Mo(CO) fragment.[9] In contrast, the ^{13}C NMR spectrum of **9** confirms the retention of two Mo-bound (239.0 and 238.7 ppm) and three Re-bound carbonyls (199.6, 196.5 and 195.2 ppm), with the expected couplings to the P atom depending on their relative positioning to it (*cis* or *trans*), as found for **6**, which implies that the alkenyl ligand in **9** must be σ-bound to Mo and π-bound to Re. However, the ^{31}P chemical shifts of compounds **9** and **6** are dramatically different from each other

(211.4 vs. 52.6 ppm). Moreover, although the IR spectrum of **9** displays a strong high-frequency C–O stretch characteristic of pyramidal $Re(CO)_3$ oscillators, as also found in **6**, the overall pattern of the C–O stretches is significantly different from that of **6**, particularly as concerning the separation between the two more energetic stretches in each case (32 cm^{-1} for **6** but 70 cm^{-1} for **9**). All of this suggests that the relative conformation of the $Mo(CO)_2$ and $Re(CO)_3$ fragments might be different in these two compounds.

To solve the above uncertainty we carried out DFT calculations on possible conformations for the alkenyl-bridged complex **9**, and found indeed that the conformation observed for **6** (type **A** structure) is not the most stable one when replacing the SPh group with an alkenyl ligand (Figure 4). Instead, a more stable conformation (by 27 kJ/mol) is reached by a 180° rotation of the $MoCp(CO)_2$ fragment around the intermetallic bond, which leaves the $Mo(CO)_2$ and $Re(CO)_3$ oscillators in a sort of *anti* conformation, thus justifying the different patterns of the corresponding C–O stretches (see the SI). In a way, the structure of **9** can be related to that of the ammonia complex [MoReCp(μ-H)(μ-PCy_2)$(CO)_5(NH_3)$],[8] if we replace the bridging hydride with the alkenyl α-carbon and the terminal ammonia with the CH_2 group. Indeed, the C–O stretches of these two complexes are very similar (cf. 2003 (s), 1935 (vs), 1904 (s), 1883 (s), and 1856 (m) cm^{-1} for the NH_3 complex).

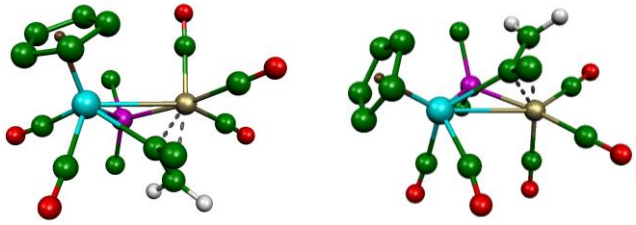

Figure 4. DFT-optimized structure of compound **9** (left) and an isomer with a type **A** structure (right), with Cy and *p*-tol groups (except their C^1 atoms), and most H atoms omitted. Relative Gibbs free energies at 298 K were 0 and + 27 kJ/mol respectively.

Structure of the Formyl-alkenyl Complexes 10. The structure of the minor isomer (*anti*) of compound **10** in the crystal (Figure 5 and Table 5) is built from MoCp(CO) and pyramidal $Re(CO)_3$ fragments bridged by a phosphanide ligand, and by an alkenyl ligand σ-bound to Re (Re1–C7 = 2.24(1) Å) and π-bound to Mo (Mo–C7 = 2.17(1), Mo–C6 = 2.25(1) Å), which also bears a formyl group *O*-bound to Re (Re–O = 2.160(6) Å), thus completing an octahedral environment around this atom. In all, this electron-precise structure (Mo–Re = 2.970(1) Å) can be viewed as a type **B** [MoReCp(μ-PCy_2)(μ-X)$(CO)_5$] structure with the alkenyl group at the bridging X position and the formyl group playing the role of an axial Re-bound carbonyl, while the phosphanide ligand is more tightly bound to molybdenum (Δd ca. 0.10 Å), to better balance the different electron counts of the metal fragments. The Mo-bound carbonyl and the Re-bound O atom of the formyl group are positioned at opposite sides of the average plane defined by the central MoPReC7 ring of the molecule, which now is almost perfectly flat (P–Mo–Re–C7 176°). The overall structure thus results fully analogous to the one recently determined for the DMAD-derived alkenyl complex [MoReCp{μ-η^2:κ_C,κ_O-C(CO_2Me)CH(CO_2Me)}(μ-PCy_2)$(CO)_4$], which displays a carboxylate substituent *O*-bound to Re (2.217(4) Å) and a similar intermetallic separation of 2.9943(5) Å. However, the π-bonding of the alkenyl ligand in ***anti*-10** seems stronger, as judged from its shorter Mo–C_β distance (2.25(1) vs. 2.322(7) Å for the DMAD derivative). M–C_β lengths were also higher for the other two complexes with alkenyl ligands bridging over Mo–Re or W–Re bonds which have been structurally characterized so far: the mentioned [MoReCp(μ-κ^1:η^2-CRCHR)(μ-PCy_2)$(CO)_5$] (π-bound to Mo; Mo–C_β = 2.309(3) A),[9] and the cluster [W_2ReCp*(μ-κ^1:η^2-CHCHPh)(O)$(CO)_8$] (π-bound to Re; Re–C_β = 2.393 A).[17c] We finally note that dimensions within the formyl-alkenyl chain in ***anti*-10** are comparable to those recently measured for the related dimolybdenum complexes *cis*- and *trans*-[Mo_2Cp_2\{μ-$\kappa^2_{C,O}$:$\eta^2_{C,C}$-CHC(^{t}Bu)C(O)H\}\{μ-P(CH_2CMe_2)$C_6H_2{}^t Bu_2$\}$(CO)_2$], which are formed in a multistep process taking place upon photolysis of the phosphinidene complex [Mo_2Cp_2(μ-PR)$(CO)_4$] with HC≡C^{t}Bu,[26] a matter to be further discussed below (R = 2,4,6-$C_6H_2{}^t Bu_3$).

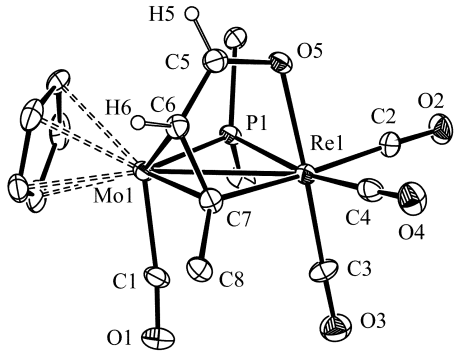

Figure 5. ORTEP drawing (30% probability) of ***anti*-10**, with Cy and *p*-tol groups (except their C^1 atoms), and most H atoms omitted.

Table 5. Selected Bond Lengths (Å) and Angles (°) for *anti*-10.

Mo1–Re1	2.970(1)	Mo1–P1–Re1	75.7(1)
Mo1–P1	2.365(2)	Mo1–C7–Re1	84.6(3)
Re1–P1	2.470(2)	P1–Mo1–C1	96.6(3)
Mo1–C1	1.98(1)	P1–Mo1–C6	108.0(2)
Mo1–C7	2.17(1)	P1–Mo1–C7	102.4(3)
Re1–C7	2.24(1)	P1–Re1–C2	89.3(3)
Mo1–C6	2.25(1)	P1–Re1–C3	97.3(3)
Re1–O5	2.160(6)	P1–Re1–C4	170.6(3)
Re1–C2	1.93(1)	P1–Re1–C7	97.0(3)
Re1–C3	1.91(1)	P1–Re1–O5	81.7(2)
Re1–C4	1.96(1)	Re1–O5–C5	110.3(6)
C5–O5	1.30(1)	O5–C5–C6	123.1(8)
C5–C6	1.40(1)	C5–C6–C7	119.4(8)
C6–C7	1.45(1)	C6–C7–C8	121.7(8)
C7–C8	1.47(1)		

Spectroscopic data in solution for ***syn*-10** and ***anti*-10** (Table 1 and Experimental Section) are similar to each other and consistent with the structure found for the *anti* isomer in the crystal. The formyl-alkenyl ligand gives rise to diagnostic ^{13}C NMR resonances at ca. 56 (CH), 160 (μ-C) and 205 ppm (C(O)H), with the formyl group giving rise also to a strongly deshielded ^{1}H NMR resonance at ca. 9 ppm (cf. 8.6 ppm in the mentioned Mo_2 complexes). Both isomers also display one carbonyl ligand bound to Mo (δ_C ca. 240 ppm) and three ones at the Re atom (δ_C ca. 198 ppm). The IR spectrum in both cases displays a strong high-frequency C–O stretch at 2020 cm^{-1}, characteristic of pyramidal $Re(CO)_3$ oscillators, but the lowest-frequency band at ca. 1890 cm^{-1}, likely having the largest contribution from the Mo(CO) fragment, has very different relative intensity in both isomers. It is very strong in the *syn* isomer but rather weak in the *anti* isomer, which is in agreement with the distinct relative orientation of the Mo(CO) and $Re(CO)_3$ oscillators in these two isomers.[10]

Scheme 5. Proposed Steps for the Thermal Rearrangement of Compound 9

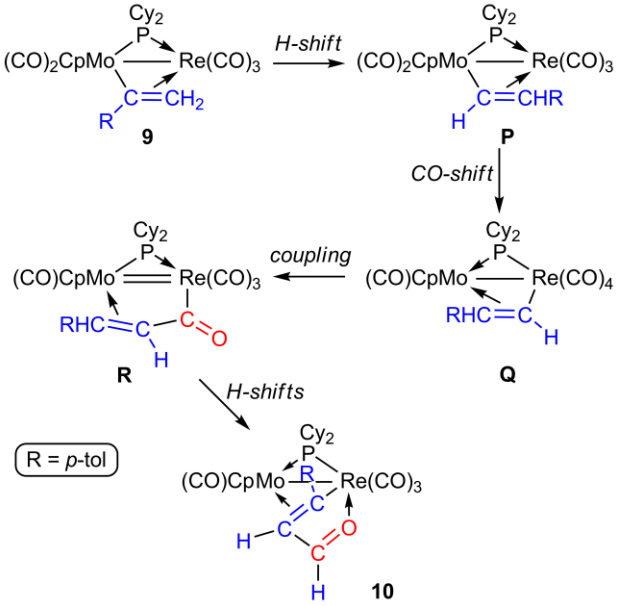

Elemental Steps in the Formation of the Formyl-alkenyl Ligand. The building of the bridging hydrocarbyl ligand found in complexes **10** necessarily is a multistep process involving alkenyl-carbonyl coupling and H shifts at some stages, but the exact sequence of events is difficult to grasp. It has been previously shown that related formyl-alkenyl complexes $[Mo_2Cp_2(\mu\text{-}PPh_2)\{\mu\text{-}\kappa^2_{C,O}\text{:}\eta^2_{C,C}\text{-}CRCRC(O)H\}(CO)_2]$ can be prepared through the thermal rearrangement of the corresponding alkyne complexes $[Mo_2Cp_2(\mu\text{-}\eta^2\text{:}\eta^2\text{-}C_2R_2)(PPh_2H)(CO)_3]$ (R= H, CO_2Me),[27,28] and similar rearrangements are suspected to be at the origin of the phosphinidene derivatives $[Mo_2Cp_2\{\mu\text{-}\kappa^2_{C,O}\text{:}\eta^2_{C,C}\text{-}CHC(^tBu)C(O)H\}\{\mu\text{-}P(CH_2CMe_2)C_6H_2{}^tBu_2\}(CO)_2]$ mentioned above.[26] In these cases, an alkenyl ligand might be also involved at an intermediate stage, since the latter might be readily formed following from P–H bond cleavage at a PHR_2 ligand (to form the phosphanide ligand) and coupling of the resulting hydride ligand with the bridging alkyne. That would yield Mo_2 intermediates bridged by phosphanide and alkenyl ligands akin to compound **9**, these preceding the alkenyl-carbonyl coupling step. In the case of **9**, the latter coupling is unlikely to proceed directly from **9**, since this would render a CO group bound to the C(*p*-tol) atom, while the actual structure of **10** displays instead a C(*p*-tol)–CH–C(O)H chain. To achieve the observed coupling, we propose that the rearrangement of **9** first involves a 2,1-H shift to yield a β-substituted alkenyl intermediate **P** (Scheme 5). This is a spontaneous rearrangement observed at the unsaturated homonuclear complexes $[M_2Cp_2\{\mu\text{-}\kappa^1\text{:}\eta^2\text{-}C(p\text{-tol})CH_2\}(\mu\text{-}PCy_2)(CO)_2]$ (M = Mo, W),[23] and it has been also observed in other alkenyl-bridged complexes upon thermal activation.[29,30] Intermediate **P** might then undergo a carbonyl rearrangement similar to the isomerization discussed for the thiolate complexes (**6**→**7**), now to yield an intermediate **Q** having the alkenyl ligand σ bound to a $Re(CO)_4$ fragment, at which carbonyl-alkenyl coupling might readily occur in a conventional migratory insertion step. That would yield a new intermediate **R** which is electronically unsaturated, since the newly generated acyl-alkene ligand only provides the dimetal centre with three electrons. The five-electron donor formyl-alkenyl ligand eventually found in complex **10** might then be formed through 1,2 shifts of both H atoms at the hydrocarbyl ligand of this intermediate.

CONCLUDING REMARKS

The unsaturated nature of anion **1** enables the addition of simple donors L under mild conditions, to give electron-precise anions of type $[MoReCp(\mu\text{-}PCy_2)(CO)_5L]^-$ having the ligand L bound to Re and generally positioned *cis* to the PCy_2 bridge [L = CO, HSPh, HC_2(p-tol)] according to the spatial orientation of the LUMO in **1**, except for the bulkier ligand PPh_2H, which eventually occupies a less crowded position *trans* to the PCy_2 bridge. E–H bond activation in the added ligand L takes place only in the neutral derivatives formed upon protonation of these saturated anions, which incidentally is a spontaneous process in the HSPh reaction thanks to the significant Brönsted acidity of this reagent. In that case, dehydrogenation takes place easily at the corresponding thiol complex $[MoReCp(\mu\text{-}H)(\mu\text{-}PCy_2)(CO)_5(HSPh)]$ to give the thiolate derivative $[MoReCp(\mu\text{-}PCy_2)(\mu\text{-}SPh)(CO)_5]$, which displays a quite puckered central MoPReS ring. The analogous reaction on the PPh_2H complex does not proceed thermally, but it can be induced photochemically to give a related PPh_2-bridged complex $[MoReCp(\mu\text{-}PCy_2)(\mu\text{-}PPh_2)(CO)_5]$ which, however, has a different structure, with four (instead of three) carbonyls at Re and a much flatter central MoPReP ring. DFT calculations indicate that the puckered structure with a $Re(CO)_3$ fragment should be generally favored for $[MoReCp(\mu\text{-}PCy_2)(\mu\text{-}X)(CO)_5]$ complexes in the absence of severe steric repulsions between the bridging ligands. In contrast to the above behavior, protonation of the anion $[MoReCp(\mu\text{-}PCy_2)(CO)_5L]^-$ when L = HC_2(p-tol) seems to take place at the terminal carbon of the alkyne to give an unstable alkenyl-bridged complex $[MoReCp\{\mu\text{-}\kappa^1\text{:}\eta^2\text{-}C(p\text{-tol})CH_2\}(\mu\text{-}PCy_2)(CO)_5]$, which readily undergoes alkenyl-carbonyl coupling and different H-shifts to eventually yield a product bearing a formyl-alkenyl ligand bridging the heterometallic center in a $\kappa^2_{C,O}\text{:}\eta^2_{C,C}$- fashion.

EXPERIMENTAL SECTION

General Procedures and Starting Materials. All manipulations and reactions were carried out under an argon (99.995%) atmosphere

using standard Schlenk techniques. Solvents were purified according to literature procedures, and distilled prior to use.[31] Compound [MoReCp(μ-PCy$_2$)(μ-PPh$_2$)(CO)$_5$], and tetrahydrofuran suspensions of Na[MoReCp(μ-PCy$_2$)(CO)$_5$] (**1-Na**), were prepared from [MoReCp(μ-H)(μ-PCy$_2$)(CO)$_5$(NCMe)] as described recently (Cp = η^5-C$_5$H$_5$),[9] and all other reagents were obtained from the usual commercial suppliers and used as received, unless otherwise stated. Petroleum ether refers to that fraction distilling in the range 338-343 K. Photochemical experiments were performed using jacketed Pyrex Schlenk tubes cooled by tap water (ca. 288 K). A 400 W medium-pressure mercury lamp placed ca. 1 cm away from the Schlenk tube was used for these experiments. Chromatographic separations were carried out using jacketed columns refrigerated by tap water (ca. 288 K) or by a closed 2-propanol circuit, kept at the desired temperature with a cryostat. Commercial aluminum oxide (activity I, 70-290 mesh) was degassed under vacuum prior to use. The latter was mixed afterwards under argon with the appropriate amount of water to reach activity IV. IR stretching frequencies of CO ligands were measured in solution using CaF_2 windows, and are given in cm^{-1}. NMR spectra were routinely recorded at 295 K unless otherwise stated. Chemical shifts (δ) are given in ppm, relative to internal tetramethylsilane (^{1}H, ^{13}C) or external 85% aqueous H_3PO_4 (^{31}P). Coupling constants (J) are given in Hertz.

Preparation of Tetrahydrofuran Suspensions of Na[MoReCp(μ-PCy$_2$)(CO)$_5$] (1-Na). For this we used a slight modification of the method recently reported by us,[9] in order to get solutions free from acetonitrile. In a typical experiment, a solution of [MoReCp(μ-H)(μ-PCy$_2$)(CO)$_5$(NCMe)] (0.015 g, 0.021 mmol) in tetrahydrofuran (6 mL) was stirred with an excess of 0.5% Na-amalgam (ca. 1 mL, 3 mmol) for 15 min to give a green-yellowish suspension that was transferred to another Schlenk tube using a cannula. The solvent was then removed under vacuum and tetrahydrofuran (4 mL) was added to the residue. The suspension thus obtained contains essentially pure **1-Na**, and this product was assumed to be formed in ca. 100% yield. Spectroscopic data for this product were identical to those reported originally for this salt.[8]

Preparation of Tetrahydrofuran Solutions of Na[MoReCp(μ-PCy$_2$)(CO)$_5$(PPh$_2$H)] (2-Na). Neat PPh$_2$H (4 μL, 0.023 mmol) was added to a suspension of compound **1-Na** (ca. 0.021 mmol) in tetrahydrofuran (4 mL), and the mixture was stirred for 5 min to give a yellow solution shown (by NMR) to contain compound **2-Na** as major product. Unfortunately, all attempts to isolate this air-sensitive product as a pure solid led to its progressive decomposition. IR and ^{31}P NMR data for this compound are collected in Table 1.

Preparation of *mer*-[MoReCp(μ-H)(μ-PCy$_2$)(CO)$_5$(PPh$_2$H)] (3). Solid $(NH_4)PF_6$ (0.015 g, 0.092 mmol) was added to a crude solution containing ca. 0.021 mmol of **2-Na**, prepared *in situ* as described above, and the mixture was stirred at room temperature for 5 min to give a yellow solution. The solvent was then removed under vacuum, the residue was extracted with petroleum ether, and the extracts were chromatographed on alumina at 288 K. Elution with petroleum ether gave a yellow fraction yielding, after removal of solvents, compound **3** as a yellow microcrystalline solid (0.016 g, 87%). Anal. Calcd for C$_{34}$H$_{39}$MoO$_5$P$_2$Re: C, 46.84; H, 4.51. Found: C, 46.55; H, 4.32. ^{1}H NMR (300.13 MHz, CD$_2$Cl$_2$): δ 7.78 (m, 2H, Ph), 7.65 (m, 2H, Ph), 7.47 (m, 6H, Ph), 7.44 (dd, $^1J_{HP}$ = 358, $^3J_{HH}$ = 1, 1H, PH), 4.88 (s, 5H, Cp), 2.60 (m, 1H, Cy), 2.41 (m, br, 1H, Cy), 2.19 (m, 1H, Cy), 2.10-1.06 (m, 19H, Cy), –13.07 (ddd, $^2J_{HP}$ = 18, 16, $^3J_{HH}$ = 1, 1H, μ-H).

Preparation of [MoReCp(μ-O)(μ-PCy$_2$)(μ-PPh$_2$)(CO)$_3$] (4). A toluene solution (4 mL) of complex [MoReCp(μ-PCy$_2$)(μ-PPh$_2$)(CO)$_5$] (0.020 g, 0.023 mmol) was refluxed for 2 h to give a dark green solution. The solvent was then removed under vacuum, the residue was extracted with dichloromethane/petroleum ether (1/1), and the extracts were chromatographed on alumina at 253 K. Elution with the above solvent mixture gave a dark green fraction yielding, after removal of solvents, compound **4** as an air-sensitive, dark green microcrystalline solid (0.017 g, 89%). The crystals used in the X-ray diffraction study were grown through the slow diffusion of a layer of petroleum ether into a concentrated dichloromethane solution of the complex at 253 K. Anal. Calcd for C$_{32}$H$_{37}$MoO$_4$P$_2$Re: C, 46.32; H, 4.49. Found: C, 46.05; H, 4.12. ^{1}H NMR (300.13 MHz, CD$_2$Cl$_2$): δ 7.57-7.38 (m, 5H, Ph), 7.19-7.07 (m, 3H, Ph), 6.87 (m, 2H, Ph), 5.73 (s, 5H, Cp), 2.08-0.75 (m, 20H, Cy), 0.54, 0.16 (2m, 2 x 1H, Cy). ^{13}C{^{1}H} NMR (100.63 MHz, CD$_2$Cl$_2$): δ 198.0 (dd, $^2J_{CP}$ = 37, 7, ReCO), 196.7 (dd, $^2J_{CP}$ = 33, 8, ReCO), 195.5 (t, $^2J_{CP}$ = 5, ReCO), 145.4 [dd, $^1J_{CP}$ = 32, $^3J_{CP}$ = 2, C^1(Ph)], 136.4 [d, $^2J_{CP}$ = 9, C^2(Ph)], 134.5 [d, $^1J_{CP}$ = 52, C^1(Ph)], 131.7 [d, $^2J_{CP}$ = 12, C^2(Ph)], 130.5 [d, $^4J_{CP}$ = 1, C^4(Ph)], 128.9, 128.2 [2d, $^3J_{CP}$ = 11, C^3(Ph)], 128.0 [d, $^4J_{CP}$ = 3, C^4(Ph)], 95.3 (s, Cp), 43.0 [d, $^1J_{CP}$ = 23, C^1(Cy)], 38.0 [d, $^1J_{CP}$ = 12, C^1(Cy)], 34.1 [d, $^2J_{CP}$ = 5, C^2(Cy)], 33.7 [d, $^2J_{CP}$ = 2, C^2(Cy)], 33.6 [d, $^2J_{CP}$ = 5, C^2(Cy)], 33.4 [d, $^2J_{CP}$ = 2, C^2(Cy)], 27.8, 27.7 [2d, $^3J_{CP}$ = 11, C^3(Cy)], 27.5 [d, $^3J_{CP}$ = 12, C^3(Cy)], 27.4 [d, $^3J_{CP}$ = 14, C^3(Cy)], 26.7, 25.9 [2s, C^4(Cy)].

Preparation of Tetrahydrofuran Solutions of [MoReCp(μ-H)(μ-PCy$_2$)(CO)$_5$(HSPh)] (5). Neat thiophenol (4 μL, 0.039 mmol) was added to a suspension of compound **1-Na** (ca. 0.021 mmol) in tetrahydrofuran (4 mL), and the mixture was stirred for 5 min to give a pale green solution shown (by NMR) to contain compound **5** as a ca. 3:2 mixture of *anti* and *syn* isomers (see text). All attempts to isolate this air-sensitive product as a pure solid led to its progressive transformation into compound **6**. ^{1}H NMR (300.13 MHz, THF-d_8, isomer mixture): δ 7.80-6.31 (m, 5H, *syn* and *anti*), 5.21 (s, 5H, Cp, *syn*), 5.18 (s, 5H, Cp, *anti*), 2.93-0.92 (m, 22H, Cy, *syn* and *anti*), 0.10 (s, 1H, SH, *anti*), 0.04 (s, 1H, SH, *syn*), –10.97 (d, $^2J_{HP}$ = 20, 1H, μ-H, *syn*), –12.03 (d, $^2J_{HP}$ = 22, 1H, μ-H, *anti*).

Preparation of [MoReCp(μ-PCy$_2$)(μ-SPh)(CO)$_5$] (6). The solvent was removed under vacuum from a crude solution containing ca. 0.030 mmol of compound **5**, prepared *in situ* as described above, the residue was dissolved in toluene (5 mL), and the solution was stirred at room temperature for 1 h to give an orange solution containing compound **6** as the unique product. The solvent was then removed under vacuum, the residue was extracted with dichloromethane/petroleum ether (1/4), and the extracts were chromatographed on alumina at 288 K. Elution with the same solvent mixture gave a yellow fraction yielding, after removal of solvents, compound **6** as an orange microcrystalline solid (0.020 g, 84%). The crystals used in the X-ray diffraction study were grown through the slow diffusion of layers of diethyl ether and petroleum ether into a concentrated dichloromethane solution of the complex at 253 K. Anal. Calcd for C$_{28}$H$_{32}$MoO$_5$PReS: C, 42.37; H, 4.06; S, 4.04. Found: C, 42.69; H, 4.38; S, 4.28. ν(CO) (petroleum ether): 2020 (vs), 1990 (m), 1934 (s), 1915 (s), 1901 (m). ^{1}H NMR (400.13 MHz, CD$_2$Cl$_2$): δ 7.41 (m, 2H, Ph), 7.22 (m, 3H, Ph), 5.74 (s, 5H, Cp), 2.21-1.06 (m, 22H, Cy). ^{13}C{^{1}H} NMR (100.63 MHz, CD$_2$Cl$_2$): δ 234.8 (d, $^2J_{CP}$ = 11, MoCO), 228.0 (d, $^2J_{CP}$ = 2, MoCO), 200.5 (d, $^2J_{CP}$ = 39, ReCO), 198.8 (d, $^2J_{CP}$ = 4, ReCO), 198.3 (d, $^2J_{CP}$ = 8, ReCO), 141.5 [d, $^1J_{CP}$ = 20, C^1(Ph)], 133.4, 128.5 [2s, C^{2,3}(Ph)], 127.2 [s, C^4(Ph)], 90.6 (s, Cp), 46.7 [d, $^1J_{CP}$ = 20, C^1(Cy)], 38.9 [s, C^2(Cy)], 37.9 [d, $^2J_{CP}$ = 1, C^2(Cy)], 36.6 [d, $^1J_{CP}$ = 9, C^1(Cy)], 34.3 [d, $^2J_{CP}$ = 2, C^2(Cy)], 33.7 [d, $^2J_{CP}$ = 5, C^2(Cy)], 28.9 [d, $^3J_{CP}$ = 12, C^3(Cy)], 28.8 [d, $^3J_{CP}$ = 11, C^3(Cy)], 28.2 [d, $^3J_{CP}$ = 10, C^3(Cy)], 28.0 [d, $^3J_{CP}$ = 12, C^3(Cy)], 26.3, 26.2 [2s, C^4(Cy)].

Preparation of [MoReCp(μ-PCy$_2$)(μ-SPh)(1κ-CO)(CO)$_4$] (7). A toluene solution (6 mL) of compound **6** (0.020 g, 0.025 mmol) was irradiated with visible-UV light at 288 K for 20 min to give a brown solution shown (by NMR) to contain a ca 3:2 mixture of compounds **7** and **6**. All attempts to isolate compound **7** form these mixtures resulted in its progressive transformation into the parent compound **6** (see text). The NMR data for this product were obtained by removing the solvent from the reaction mixture and dissolving the residue in toluene-d_8 at 253 K. ^{1}H NMR (400.13 MHz, toluene-d_8, 233 K): δ 8.12 (d, J_{HH} = 7, 2H, Ph), 6.87 (m, 3H, Ph), 4.94 (s, 5H, Cp), 2.35-0.76 (m, 22H, Cy). ^{13}C{^{1}H} NMR (100.63 MHz, toluene-d_8, 233 K): δ 235.5 (s, MoCO), 188.7 (s, 2ReCO), 181.5, 181.2 (2s, ReCO), 144.4 [s, C^1(Ph)], 133.4, 132.0 [2s, C^{2,3}(Ph)], 126.4 [s, C^4(Ph)], 89.2 (s, Cp), 53.3 [d, $^1J_{CP}$ = 19, C^1(Cy)], 46.2 [d, $^1J_{CP}$ = 12, C^1(Cy)], 36.9, 35.3, 33.8, 33.2 [4s, C^2(Cy)], 29.2-27.3 [m, 4C^3(Cy)], 26.4, 26.1 [2s, C^4(Cy)] ppm.

Preparation of Tetrahydrofuran Solutions of Na[MoReCp(μ-PCy$_2$)(CO)$_5${η^2-HC$_2$(*p*-tol)}] (8-Na). Neat HC≡C(*p*-tol) (20 μL,

0.158 mmol) was added to a suspension of compound **1-Na** (ca. 0.060 mmol) in tetrahydrofuran (4 mL), and the mixture was stirred in a Schlenk tube equipped with a Young's valve for 20 min to give a red solution shown (by NMR) to contain compound **8-Na** as major product. All attempts to isolate this air-sensitive product as a pure solid led to its progressive decomposition. ^{1}H NMR (400.13 MHz, THF-d_8, 295 K): δ 7.30 (vbr, 2H, C_6H_4), 7.16 (br, 2H, C_6H_4), 5.96 (s, 1H, CH), 4.98 (s, 5H, Cp), 2.75-1.25 (m, 22H, Cy), 2.45 (s, 3H, Me). ^{1}H NMR (400.13 MHz, THF-d_8, 253 K): δ 7.23 (d, $^3J_{HH}$ = 7, 1H, C_6H_4), 7.15, 7.12 (AB system, $^3J_{HH}$ = 8, 2 x 1H, C_6H_4), 5.99 (s, 1H, CH), 4.98 (s, 5H, Cp), 2.77-1.17 (m, 22H, Cy), 2.46 (s, 3H, Me); the fourth C_6H_4 resonance was obscured by the 7.50 ppm resonance of the excess alkyne present in the reaction mixture. ^{13}C{^{1}H} NMR (100.63 MHz, THF-d_8, 253 K): δ 241.8 (d, $^2J_{CP}$ = 13, MoCO), 224.5 (d, $^2J_{CP}$ = 6, MoCO), 203.8 (d, $^2J_{CP}$ = 8, ReCO), 202.4 (d, $^2J_{CP}$ = 27, ReCO), 197.4 (d, $^2J_{CP}$ = 4, ReCO), 153.6 [s, C^1(C_6H_4)], 134.0 [s, C^2(C_6H_4)], 133.4 [s, C^4(C_6H_4)], 129.9 [s, C^2(C_6H_4)], 127.7, 119.0 [2s, C^3(C_6H_4)], 126.0 (s, *C*≡CH), 93.3 (s, Cp), 76.6 (s, C≡*C*H), 59.6 [d, $^1J_{CP}$ = 13, C^1(Cy)], 46.7 [d, $^1J_{CP}$ = 19, C^1(Cy)], 38.4 [d, $^2J_{CP}$ = 3, C^2(Cy)], 36.4, 36.0, 35.5 [3s, C^2(Cy)], 29.6, 29.2, 29.03 [3d, $^3J_{CP}$ = 9, C^3(Cy)], 29.02 [d, $^3J_{CP}$ = 12, C^3(Cy)], 27.5, 27.4 [2s, C^4(Cy)], 21.2 (s, Me).

Preparation of [MoReCp{μ-κ^1:η^2-C(*p*-tol)CH$_2$}(μ-PCy$_2$)(CO)$_5$] (9). Solid $(NH_4)PF_6$ (0.020 g, 0.123 mmol) was added to a crude solution containing ca. 0.060 mmol of **8-Na**, prepared *in situ* as described above, and the mixture was stirred at room temperature for 2 min to give a maroon solution containing compound **9** as major product, along with small amounts of the known complex [MoRe(μ-H)(μ-PCy$_2$)(CO)$_6$].[24] Compound **9** turned to be thermally unstable in solution at room temperature, it readily decomposing under these conditions to give a ca. 1:6:2 mixture of the above hexacarbonyl complex and the isomers ***syn*-10** and ***anti*-10** after 30 min. NMR data for **9** were recorded by just removing the solvent from a freshly prepared reaction mixture and dissolving the residue in the appropriate solvent, preferentially at low temperature. ^{1}H NMR (400.54 MHz, CD_2Cl_2, 253 K): δ 6.35, 3.16 (2s, 2 x 1H, C=CH$_2$), 4.94 (s, 5H, Cp), 2.81-0.97 (m, 22H, Cy); the resonances of the *p*-tol group were obscured by those of the excess alkyne present in the crude reaction mixture. ^{13}C{^{1}H} NMR (100.63 MHz, CD_2Cl_2, 253 K): δ 239.0 (s, MoCO), 238.7 (d, $^2J_{CP}$ = 10, MoCO), 199.6 (s, br, ReCO), 196.5 (d, $^2J_{CP}$ = 27, ReCO), 195.2 (d, $^2J_{CP}$ = 6, ReCO), 184.5 (s, br, μ-C), 148.9 [s, C^1(C_6H_4)], 134.9 [s, C^4(C_6H_4)], 132.8, 129.9, 128.1, 119.8 [4s, br, C^{2,3}(C_6H_4)], 93.4 (s, Cp), 75.3 (s, C=*C*H$_2$), 57.5, 45.9 [2d, $^1J_{CP}$ = 15, C^1(Cy)], 37.9 [d, $^2J_{CP}$ = 4, C^2(Cy)], 36.3 [d, $^2J_{CP}$ = 2, C^2(Cy)], 34.8 [s, 2C^2(Cy)], 29.1-28.0 [m, 4C^3(Cy)], 26.6 [s, 2C^4(Cy)], 21.7 (s, CH$_3$).

Preparation of [MoReCp{μ-η^2:$\kappa^2_{C,O}$-C(*p*-tol)CHC(O)H}(μ-PCy$_2$)(CO)$_4$] (10). A crude solution of compound **9** (ca. 0.060 mmol), prepared as described above, was stirred at room temperature for 30 min. The solvent was then removed under vacuum, the residue was extracted with dichloromethane/petroleum ether (1/5), and the extracts were chromatographed on alumina at 253 K. Elution with the above solvent mixture gave an orange fraction containing a small amount of the known complex [MoRe(μ-H)(μ-PCy$_2$)(CO)$_6$]. [24] Elution with dichloromethane/petroleum ether (1/3) gave an orange fraction yielding, after removal of solvents, isomer ***syn*-10** as an orange microcrystalline solid (0.026 g, 54%). Elution with dichloromethane/petroleum ether (3/1) gave a dark green fraction yielding analogously isomer ***anti*-10** as a green microcrystalline solid (0.014 g, 29%). The crystals used in the X-ray diffraction study were grown through the slow diffusion of a layer of petroleum ether into a concentrated dichloromethane solution of the complex at 253 K. *Data for **syn-10***: Anal. Calcd for $C_{31.5}H_{37}ClMoO_5PRe$ (***syn*-10**·1/2CH_2Cl_2): C, 44.82; H, 4.42. Found: C, 44.83; H, 4.30. ^{1}H NMR (400.13 MHz, CD_2Cl_2): δ 9.22 [s, 1H, C(O)H], 7.31 (d, $^3J_{HH}$ = 7, 2H, C_6H_4), 7.17 (d, $^3J_{HH}$ = 7, 2H, C_6H_4), 4.97 (d, $^3J_{HH}$ = 1, 1H, CH), 4.92 (s, 5H, Cp), 2.42 (m, 2H, Cy), 2.38 (s, 3H, CH$_3$), 2.17-1.12 (m, 20H, Cy). ^{13}C{^{1}H} NMR (100.63 MHz, CD_2Cl_2): δ 243.8 (d, $^2J_{CP}$ = 16, MoCO), 212.1 [s, C(O)H], 198.9 (d, $^2J_{CP}$ = 9, ReCO), 197.8 (s, ReCO), 197.7 (d, $^2J_{CP}$ = 34, ReCO), 175.5 (d, $^2J_{CP}$ = 2, μ-C), 152.6 [s, C^1(C_6H_4)], 136.2 [s, C^4(C_6H_4)], 129.4, 120.7 [2s, br, C^{2,3}(C_6H_4)], 93.8 (s, Cp), 57.6 [d, $^1J_{CP}$ = 19, C^1(Cy)], 57.0 (s, CH), 47.0 [d, $^1J_{CP}$ = 16, C^1(Cy)], 37.4 [d, $^2J_{CP}$ = 6, C^2(Cy)], 36.0, 35.1 [2d, $^2J_{CP}$ = 4, C^2(Cy)], 33.4 [s, C^2(Cy)], 28.9 [d, $^3J_{CP}$ = 10, C^3(Cy)], 28.7, 28.6 [2d, $^3J_{CP}$ = 11, C^3(Cy)], 28.4 [d, $^3J_{CP}$ = 12, C^3(Cy)], 26.7 [s, 2C^4(Cy)], 21.1 (s, CH$_3$). *Data for **anti-10***: Anal. Calcd for $C_{31}H_{36}MoO_5PRe$: C, 46.44; H, 4.53. Found: C, 46.15; H, 4.20. ^{1}H NMR (400.13 MHz, CD_2Cl_2): δ 8.90 [d, $^3J_{HH}$ = 2, 1H, C(O)H], 7.44 (d, $^3J_{HH}$ = 8, 2H, C_6H_4), 7.11 (d, $^3J_{HH}$ = 8, 2H, C_6H_4), 5.21 (s, 5H, Cp), 4.19 (d, $^3J_{HH}$ = 2, 1H, CH), 2.36 (s, 3H, CH$_3$), 2.47-1.20 (m, 22H, Cy). ^{13}C{^{1}H} NMR (100.63 MHz, CD_2Cl_2): δ 233.8 (d, $^2J_{CP}$ = 7, MoCO), 198.0 [s, C(O)H], 197.5 (s, ReCO), 197.4 (s, br, 2ReCO), 151.6 [s, C^1(C_6H_4)], 146.1 (s, μ-C), 134.7 [s, C^4(C_6H_4)], 129.1, 127.3 [2s, C^{2,3}(C_6H_4)], 88.0 (s, Cp), 56.1 (s, CH), 50.9 [d, $^1J_{CP}$ = 25, C^1(Cy)], 47.4 [d, $^1J_{CP}$ = 10, C^1(Cy)], 35.1 [d, $^2J_{CP}$ = 2, C^2(Cy)], 34.6 [s, 2C^2(Cy)], 33.4 [d, $^2J_{CP}$ = 3, C^2(Cy)], 29.0 [d, $^3J_{CP}$ = 11, C^3(Cy)], 28.6 [d, $^3J_{CP}$ = 10, C^3(Cy)], 28.3 [d, $^3J_{CP}$ = 12, 2C^3(Cy)], 26.5, 26.4 [2s, C^4(Cy)], 21.1 (s, CH$_3$).

X-Ray Crystal Structure Determination of Compounds 4, 6 and *anti*-10. Data collection in all cases was carried out at low temperature (130-150 K) on an Oxford Diffraction Xcalibur Nova single crystal diffractometer, using Cu-Kα radiation. Images were collected at a 62 mm fixed crystal-detector distance, using the oscillation method and variable exposure times per image. Data collection strategy was calculated with the program CrysAlis Pro CCD,[32] and data reduction and cell refinement were performed with the program CrysAlis Pro RED.[32] An empirical absorption correction was applied using the SCALE3 ABSPACK algorithm as implemented in the latter program. Using the program suite WINGX,[33]the structures were solved by Patterson interpretation and phase expansion using SHELXL2016, and refined with full-matrix least squares on F^2 using SHELXL2016.[34] In general, all non-hydrogen atoms were refined anisotropically, and all hydrogen atoms were geometrically placed and refined using a riding model, to give the residuals collected in Table S1 (see the SI). In the case of **6**, a slight disorder in one of the cyclohexyl groups was observed, but it could not be properly modeled. Compound ***anti*-10** crystallized with a dichloromethane molecule, which could be satisfactorily refined.

Computational Details. All DFT computations were carried out using the GAUSSIAN03 package,[35] in which the hybrid method B3LYP was used with the Becke three-parameter exchange functional[36] and the Lee-Yang-Parr correlation functional.[37] An accurate numerical integration grid (99,590) was used for all the calculations via the keyword Int=Ultrafine. Effective core potentials and their associated double-ζ LANL2DZ basis set were used for the metal atoms.[38] The light elements (P, S, Cl, O, C and H) were described with the 6-31G* basis.[39] Geometry optimizations were performed under no symmetry restrictions, using initial coordinates derived from X-ray data; for compounds where this information was not available, the initial coordinates were obtained by modification of the coordinates of similar complexes. Frequency analyses were performed to ensure that all the stationary points were genuine minima with no imaginary frequencies. The effect of toluene on the stability of isomers **6** and **7** in solution was modeled through the polarized-continuum-model (PCM) of Tomasi and co-workers,[40] using the gas-phase optimized structures.

ASSOCIATED CONTENT

Supporting Information

A CIF file containing full crystallographic data for compounds **4**, **6** and ***anti*-10** (CCDC 1826285 to 1826287), a PDF file containing a table with crystallographic data for the above compounds, spectra for all new compounds, and DFT-computed structures and energies of compounds [MoReCp(μ-PCy$_2$)(μ-X)(CO)$_5$] (X= PPh$_2$, SPh, Cl, C(*p*-tol)CH$_2$), and an XYZ file including the Cartesian coordinates for all computed species. The Supporting Information is available free of charge on the ACS Publications website.

AUTHOR INFORMATION

Corresponding Authors

E-mail: garciavdaniel@uniovi.es (D.G.-V.), mara@uniovi.es (M.A.R.).

Notes

The authors declare no competing financial interest.

ACKNOWLEDGMENT

This work is dedicated to Prof. Ernesto Carmona, a brilliant scientist, a charming person, and a friend, in recognition of his outstanding contribution to modern organometallic chemistry.

We thank the MINECO of Spain and FEDER for financial support (Project CTQ2015-63726-P) and a grant (to E. H.), the Consejería de Educación of Asturias (Project GRUPIN14-011) for financial support, and the CMC and X-Ray units of the Universidad de Oviedo for access to computing facilities and acquisition of diffraction data, respectively.

REFERENCES

(1) (a) Cotton, F. A.; Wilkinson, G. *Advanced Inorganic Chemistry, 5th ed.*; Wiley: New York, 1988, Chapter 22. (b) Ellis, J. E. Highly Reduced Metal Carbonyl Anions: Synthesis, Characterization, and Chemical Properties. *Adv. Organomet. Chem.* **1990**, *31*, 1-51. (c) Ellis, J. E. Adventures with substances containing metals in negative oxidation states. *Inorg. Chem.* **2006**, *45*, 3167-3186, and references therein.

(2) (a) Liu, X. Y.; Riera, V.; Ruiz, M. A.; Lanfranchi, M; Tiripicchio, A. Manganese-gold and -silver mixed-metal clusters derived from the unsaturated binuclear complex $[Mn_2(CO)_6(\mu\text{-}Ph_2PCH_2PPh_2)]^{2-}$ (*Mn*=*Mn*) and related anions. *Organometallics* **2003**, *22*, 4500, and references therein.

(3) Seyferth, D.; Brewer, K. S.; Wood, T. G.; Cowie, M.; Hilts, R. W. Synthesis and Reactions of the $[(\mu\text{-}PPh_2)Fe_2(CO)_6]^-$ Anion. *Organometallics* **1992**, *11*, 2570-2579.

(4) (a) García, M. E.; Melón, S.; Ramos, A.; Ruiz, M. A. Synthesis of the Triply Bonded Dimolybdenum Anions $[Mo_2(\eta^5\text{-}C_5H_5)_2(\mu\text{-}PA_2)(\mu\text{-}CO)_2]^-$ (A= Cy, Et, Ph, OEt). Unsaturated Hydride and Carbyne Derivatives. *Dalton Trans.* **2009**, 8171-8182. (b) García, M. E.; Melón, S.; Ramos, A.; Riera, V.; Ruiz, M. A.; Belletti, D.; Graiff, C.; Tiripicchio, A. A versatile and unprecedented triply bonded dimolybdenum carbonyl anion. *Organometallics* **2003**, *22*, 1983-1985.

(5) Alvarez, M. A.; Casado-Ruano, M.; García, M. E.; García-Vivó, D.; Ruiz, M. A. Structural and Chemical Effects of the P^tBu_2 Bridge at Unsaturated Dimolybdenum Complexes Having Hydride and Hydrocarbyl Ligands. *Inorg. Chem.* **2017**, *56*, 11336-11351.

(6) (a) Alvarez, M. A.; García, M. E.; García-Vivó, D.; Ruiz, M. A.; Vega, M. F. Reactions of the Unsaturated Ditungsten Anion $[W_2Cp_2(\mu\text{-}PCy_2)(\mu\text{-}CO)_2]^-$ with C- and P-based Electrophiles. *Organometallics* **2015**, *34*, 870-878. (b) Alvarez, M. A.; García, M. E.; García-Vivó, D.; Ruiz, M. A.; Vega, M. F. Synthesis and reactivity of the triply bonded binuclear anion $[W_2(\eta^5\text{-}C_5H_5)_2(\mu\text{-}PCy_2)(\mu\text{-}CO)_2]^-$: Tungsten makes a difference. *Organometallics* **2010**, *29*, 512-515.

(7) García-Vivó, D.; Ramos, A.; Ruiz, M. A. Cyclopentadienyl and related complexes of the group 6 elements having metal−metal triple bonds: synthesis, structure, bonding and reactivity. *Coord. Chem. Rev.* **2013**, *257*, 2143-2191.

(8) Alvarez, M. A.; García, M. E.; García-Vivó, D.; Huergo, E.; Ruiz, M. A. Synthesis of the Unsaturated Anions $[MoMCp(\mu\text{-}PR_2)(CO)_5]^-$ (M = Mn, R = Ph; M = Re, R = Cy): Versatile Precursors of New Heterometallic Complexes. *Eur. J. Inorg. Chem.* **2017**, 1280-1283.

(9) Alvarez, M. A.; García, M. E.; García-Vivó, D.; Huergo, E.; Ruiz, M. A. Acetonitrile Adduct $[MoReCp(\mu\text{-}H)(\mu\text{-}PCy_2)(CO)_5(NCMe)]$: A Surrogate of an Unsaturated Heterometallic Hydride Complex. *Inorg. Chem.* **2018**, *57*, 912-915.

(10) Braterman, P. S. *Metal Carbonyl Spectra*; Academic Press: London, U. K., 1975.

(11) Jameson, C. J. in *Phosphorus-31 NMR Spectroscopy in Stereochemical Analysis*; Verkade, J. G., Quin, L. D., Eds.; VCH: Deerfield Beach, FL, 1987; Chapter 6.

(12) Cordero, B.; Gómez, V.; Platero-Prats, A. E.; Revés, M.; Echevarría, J.; Cremades, E.; Barragán, F.; Alvarez, S. Covalent Radii Revisited. *Dalton Trans.* **2008**, 2832-2838.

(13) Bottomley, F.; Sutin, L. Organometallic Compounds Containing Oxygen Atoms. *Adv. Organomet. Chem.* **1988**, *28*, 339-396.

(14) For some related phosphanide-bridged complexes with terminal oxide ligands see: (a) Alvarez, M. A.; García, M. E.; García-Vivó, D.; Menéndez, S.; Ruiz, M. A. Electronic Structure and Reactivity of the Carbyne-Bridged Dimolybdenum Radical $[Mo_2(\eta^5\text{-}C_5H_5)_2(\mu\text{-}CPh)(\mu\text{-}PCy_2)(\mu\text{-}CO)]^+$. *Organometallics* **2013**, *32*, 218-231. (b) Alvarez, M. A.; García, M. E.; Riera, V.; Ruiz, M. A.; Falvello, L. R.; Bois, C. Oxidative Additions of Coordinated Ligands at Unsaturated Molybdenum and Tungsten Diphosphine-Bridged Carbonyl Dimers. 1. Decarbonylation Reactions of $[W_2(\eta^5\text{-}C_5H_5)_2(CO)_4(\mu\text{-}R_2PCH_2PR_2)]$ (R = Ph, Me). *Organometallics* **1997**, *16*, 354-364. (c) Adatia, T.; McPartlin, M.; Mays, M. J.; Morris, M. J.; Raithby, P. R. Chemistry of phosphido-bridged dimolybdenum complexes. Part 3. Reinvestigation of the reaction between $[Mo_2(\eta\text{-}C_5H_5)_2(CO)_6]$ and P_2Ph_4; *X*-ray structures of $[Mo_2(\eta\text{-}C_5H_5)_2(\mu\text{-}PPh_2)_2(CO)_2]$, $[Mo_2(\eta\text{-}C_5H_5)_2(\mu\text{-}PPh_2)_2(\mu\text{-}CO)]$, and *trans*-$[Mo_2(\eta\text{-}C_5H_5)_2(\mu\text{-}PPh_2)_2O(CO)]$. *J. Chem. Soc., Dalton Trans.* **1989**, 1555-1564. (d) Endrich, K.; Korswagen, R.; Zhan, T.; Ziegler, M. L. A $\mu_2\text{-}\eta^2$-Styryl Complex by Reaction of $Cp_2Mo_2(CO)_4$ with the Wittig Reagent $(C_6H_5)_3P{=}CH_2$. *Angew. Chem., Int. Ed. Engl.* **1982**, *21*, 919.

(15) (a) García, M. E.; García-Vivó, D.; Melón, S.; Ruiz, M. A.; Graiff, C.; Tiripicchio, A. Low-Temperature N–O Bond Cleavage in Nitrosyl Ligands Induced by the Unsaturated Dimolybdenum Anion $[Mo_2(\eta^5\text{-}C_5H_5)_2(\mu\text{-}PPh_2)(\mu\text{-}CO)_2]^-$. *Inorg. Chem.* **2009**, *48*, 9282-9293. (b) Alvarez, M. A.; García, M. E.; Ruiz, M. A.; Toyos, A. Low-Temperature N–O Bond Cleavage and Reversible N–P Bond Formation Processes in the Reactions of the Unsaturated Anions $[M_2(\eta^5\text{-}C_5H_5)_2(\mu\text{-}PCy_2)(\mu\text{-}CO)_2]^-$ (M = Mo, W) with the Nitrosyl Complex $[Re(\eta^5\text{-}C_5H_4Me)(CO)_2(NO)]^+$. *Inorg. Chem.* **2013**, *52*, 3942-3952.

(16) Pétillon, F. Y.; Schollhammer, P.; Talarmin, J.; Muir, K. W. Dinuclear molybdenum thiolato-bridged compounds: synthesis, reactivities and electrochemical studies of site-substrate interactions. *Coord. Chem. Rev.* **1998**, *178-180*, 203-247.

(17) (a) Carriedo, G. A.; Jeffery, J. C.; Stone, F. G. A. Chemistry of di- and tri-metal complexes with bridging carbene or carbyne ligands. Part 29. Synthesis of rhenium–tungsten compounds; *X*-ray crystal structures of $[ReW_2(\mu\text{-}Br)(\mu\text{-}L)(\mu\text{-}CC_6H_4Me\text{-}4)(\mu_3\text{-}CC_6H_4Me\text{-}4)(CO)_3(\eta\text{-}C_5H_5)_2]$(L = CO or O). *J. Chem. Soc., Dalton Trans.* **1984**, 1597-1603. (b) Chi, Y.; Cheng, P.-S.; Wu, H.-L.; Hwang, D.-K.; Su, P.-S.; Peng, S.-M.; Lee, G.-H. Heterometallic carbonyl cluster oxide. Formation, structure and reactivity of WRe_2 oxo-acetylide cluster compounds. *J. Chem. Soc. Chem. Commun*, **1994**, 1839-1840. (c) Chi, Y.; Wu, H.-L.; Cheng, C.-C.; Su, C.-J.; Peng, S.-M.; Lee, G.-H. Syntheses and Reactivity of Heterometallic Oxo-Acetylide Cluster Compounds. Skeletal Rearrangement and Conversion of Acetylide to Alkenyl, Alkylidene, and Allenyl Ligands on a WRe_2 Framework. *Organometallics* **1997**, *16*, 2434-2442.

(18) Darensbourg, M. Y.; Longride, E. M.; Payne, V.; Reibenspies, J.; Riordan, C. G.; Springs, J. J.; Calabrese, J. C. Isolation of Chromium(0) Thiols: Molecular Structure of $(^tBuSH)Cr(CO)_5$. *Inorg. Chem.* **1990**, *29*, 2721-2726.

(19) For some examples, see: (a) Xiao, N.; Xu, Q.; Tsubota, S.; Sun, J.; Chen, J. Novel Reactions of Cationic Carbyne Complexes of Manganese and Rhenium with Polymetal Carbonyl Anions. An Approach to Trimetal Bridging Carbyne Complexes. *Organometallics* **2002**, *21*, 2764-2772. (b) Adams, R. D.; Captain, B.; Kwon, O.-S.; Miao, S. New Disulfido Molybdenum-Manganese Complexes Exhibit Facile Addition of Small Molecules to the Sulfur Atoms. *Inorg. Chem.* **2003**, *42*, 3356-3365. (c) Adams, R. D.; Miao, S.; Smith, M. D. Light-Promoted Addition of Alkenes, Dienes, C_{60}, and Disulfur to the Disulfido Ligand in the Complex $CpMoMn(CO)_5(\mu\text{-}S_2)$. *Organometallics* **2004**, *23*, 3327-3334.

(20) Alvarez, M. A.; García, M. E.; García-Vivó, D.; Menéndez, S.; Ruiz, M. A. Reversible P–C Coupling Reactions at the Unsaturat-

ed Dimolybdenum Carbyne Complex $[Mo_2(\eta^5\text{-}C_5H_5)_2(CPh)(\mu\text{-}PCy_2)(\mu\text{-}SPh)(CO)]^+$. *Organometallics* **2012**, *31*, 7181-7190.

(21) A general trend established for $^2J_{XY}$ in complexes of the type $[MCpXYL_2]$ is that $|J_{cis}| > |J_{trans}|$. See, for instance, reference 11 and Wrackmeyer, B.; Alt, H. G.; Maisel, H. E. Ein- und zweidimensionale Multikern NMR-Spektroskopie an den isomeren Halbsandwich-Komplexen *cis*- und *trans*-$[(\eta^5\text{-}C_5H_5)W(CO)_2(H)PMe_3]$. *J. Organomet. Chem.* **1990**, *399*, 125-130.

(22) (a) Cramer, C. J. *Essentials of Computational Chemistry, 2nd Ed.*; Wiley: Chichester, UK, 2004. (b) Koch, W.; Holthausen, M. C. *A Chemist´s Guide to Density Functional Theory, 2nd Ed.*; Wiley-VCH: Weinheim, 2002.

(23) (a) Alvarez, M. A.; García, M. E.; Ramos, A.; Ruiz, M. A.; Lanfranchi, M.; Tiripicchio, A. Alkenyl Derivatives of the Unsaturated Dimolybdenum Hydride Complex $[Mo_2(\eta^5\text{-}C_5H_5)_2(\mu\text{-}H)(\mu\text{-}PCy_2)(CO)_2]$. *Organometallics* **2007**, *26*, 5454-5467. (b) Alvarez, M. A.; García, M. E.; García-Vivó; Ruiz, M. A.; Vega, M. F. Insertion and C–C Coupling Processes in Reactions of the Unsaturated Hydride $[W_2Cp_2(H)(\mu\text{-}PCy_2)(CO)_2]$ with Alkynes. *Dalton Trans.* **2016**, *45*, 5274-5289.

(24) Haupt, H. J.; Merla, A.; Florke, U. Heterometallische Clusterkomplexe der Typen $Re_2(\mu\text{-}PR_2)(CO)_8(HgY)$ und $ReMo(\mu\text{-}PR_2)(\eta^5\text{-}C_5H_5)(CO)_6(HgY)$ (R= Ph, Cy; Y= C1, $W(\eta^5\text{-}C_5H_5)(CO)_3$). *Z. Anorg. Allg. Chem.* **1994**, *620*, 999-1005.

(25) (a) Casey, C. P.; Selmeczy, A. D.; Nash, J. R.; Yi, C. S.; Powell, D. R.; Hayashi, K. Synthesis of η^3-Propargyl Rhenium Complexes. *J. Am. Chem. Soc.* **1996**, *118*, 6698-6706. (b) Casey, C. P.; Ha, Y.; Powell, D. R. Synthesis and reactions of rhenium enyne, and vinylalkenylidene complexes. *J. Organomet. Chem.* **1994**, *472*, 185-193.

(26) García, M. E.; García-Vivó, D.; Ruiz, M. A.; Sáez, D. Divergent Reactivity of the Phosphinidene Complex $[Mo_2Cp_2\{\mu\text{-}P(2,4,6\text{-}C_6H_2{}^tBu_3)\}(CO)_4]$ Toward 1-Alkynes: P–C, P–H, C–C, and C–H Couplings. *Organometallics* **2017**, *36*, 1756-1764.

(27) Adams, H.; Biebricher, A.; Gay, S. R.; Hamilton, T.; McHugh, P. E.; Morris, M. J.; Mays, M. J. Reactions of $[Mo_2(\mu\text{-}RC_2R)(CO)_4Cp_2]$ (R = CO_2Me, Cp = η-C_5H_5) with P_2Ph_4, PPh_2H and R^1SH (R^1 = Et, Pr^i, C_6H_4Me-*p* or Bu^t): stabilisation of μ-vinyl complexes by chelating substituents. *J. Chem. Soc., Dalton Trans.* **2000**, 2983-2989.

(28) Doel, G. R.; Feasey, N. D.; Knox, S. A. R.; Orpen, A. G.; Webster, J. Phosphorus–carbon bond cleavage at a dimolybdenum centre: isomerisation of $[Mo_2(CO)_3(PPh_3)(\mu\text{-}HC_2H)(\eta\text{-}C_5H_5)_2]$ to $[Mo_2(CO)_2(\mu\text{-}PPh_2)\{\mu\text{-}\eta^3\text{-}HC_2(H)C(O)Ph\}(\eta\text{-}C_5H_5)_2]$. *J. Chem. Soc., Chem. Commun.* **1986**, 542-544.

(29) Anwar, M. K.; Hogarth, G.; Senturk, O. S.; Clegg, W.; Doherty, S.; Elsegood, M. R. J. α–β Alkenyl isomerisation at diiron centres. *J. Chem. Soc., Dalton Trans.* **2001**, 341-352.

(30) Fujita, K.; Nakaguma, H.; Hanasaka, F.; Yamaguchi, R. Synthesis of a DMPM and Hydrido-Bridged Diiridium Complex, $[(Cp^*Ir)_2(\mu\text{-dmpm})(\mu\text{-}H)_2][OTf]_2$, and Its Reactivity toward Alkynes and Isocyanides. *Organometallics* **2002**, *21*, 3749-3757.

(31) Armarego, W. L. F.; Chai, C. *Purification of Laboratory Chemicals, 7th ed.*; Butterworth-Heinemann: Oxford, UK, 2012.

(32) *CrysAlis Pro*; Oxford Diffraction Ltd.: Oxford, U. K., 2006.

(33) Farrugia, L. J. WinGX suite for small-molecule single-crystal crystallography. *J. Appl. Crystallogr.* **1999**, *32*, 837-838.

(34) (a) Sheldrick, G. M. A short history of SHELX. *Acta Crystallogr., Sect. A* **2008**, *64*, 112-122. (b) Sheldrick, G. M. Crystal structure refinement with SHELXL. *Acta Crystallogr., Sect. C* **2015**, *71*, 5-8.

(35) *Gaussian 03, Revision B.02*, Frisch, M. J.; Trucks, G. W.; Schlegel, H. B.; Scuseria, G. E.; Robb, M. A.; Cheeseman, J. R.; Montgomery, Jr., J. A.; Vreven, T.; Kudin, K. N.; Burant, J. C.; Millam, J. M.; Iyengar, S. S.; Tomasi, J.; Barone, V.; Mennucci, B.; Cossi, M.; Scalmani, G.; Rega, N.; Petersson, G. A.; Nakatsuji, H.; Hada, M.; Ehara, M.; Toyota, K.; Fukuda, R.; Hasegawa, J.; Ishida, M.; Nakajima, T.; Honda, Y.; Kitao, O.; Nakai, H.; Klene, M.; Li, X.; Knox, J. E.; Hratchian, H. P.; Cross, J. B.; Bakken, V.; Adamo, C.; Jaramillo, J.; Gomperts, R.; Stratmann, R. E.; Yazyev, O.; Austin, A. J.; Cammi, R.; Pomelli, C.; Ochterski, J. W.; Ayala, P. Y.; Morokuma, K.; Voth, G. A.; Salvador, P.; Dannenberg, J. J.; Zakrzewski, V. G.; Dapprich, S.; Daniels, A. D.; Strain, M. C.; Farkas, O.; Malick, D. K.; Rabuck, A. D.; Raghavachari, K.; Foresman, J. B.; Ortiz, J. V.; Cui, Q.; Baboul, A. G.; Clifford, S.; Cioslowski, J.; Stefanov, B. B.; Liu, G.; Liashenko, A.; Piskorz, P.; Komaromi, I.; Martin, R. L.; Fox, D. J.; Keith, T.; Al-Laham, M. A.; Peng, C. Y.; Nanayakkara, A.; Challacombe, M.; Gill, P. M. W.; Johnson, B.; Chen, W.; Wong, M. W.; Gonzalez, C.; and Pople, J. A.; Gaussian, Inc., Wallingford CT, 2004.

(36) Becke, A. D. Density-functional thermochemistry. III. The role of exact exchange. *J. Chem. Phys.* **1993**, *98*, 5648-5652.

(37) Lee, C.; Yang, W.; Parr, R. G. Development of the Colle-Salvetti correlation-energy formula into a functional of the electron density. *Phys. Rev. B* **1988**, *37*, 785-789.

(38) Hay, P. J.; Wadt, W. R. Ab initio effective core potentials for molecular calculations. Potentials for potassium to gold including the outermost core orbitals. *J. Chem. Phys.* **1985**, *82*, 299-310.

(39) (a) Hariharan, P. C.; Pople, J. A. Influence of polarization functions on MO hydrogenation energies. *Theor. Chim. Acta* **1973**, *28*, 213-222. (b) Petersson, G. A.; Al-Laham, M. A. A complete basis set model chemistry. II. Open-shell systems and the total energies of the first-row atoms. *J. Chem. Phys.* **1991**, *94*, 6081-6090. (c) Petersson, G. A.; Bennett, A.; Tensfeldt, T. G.; Al-Laham, M. A.; Shirley, W. A.; Mantzaris, J. A complete basis set model chemistry. I. The total energies of closed-shell atoms and hydrides of the first-row elements. *J. Chem. Phys.* **1988**, *89*, 2193-2218.

(40) Cossi, M.; Barone, V.; Cammi, R.; Tomasi, J. Ab initio study of solvated molecules: a new implementation of the polarizable continuum model. *Chem. Phys. Lett.* **1996**, *255*, 327-335, and references therein

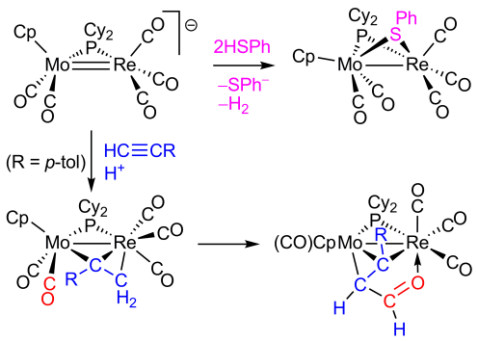

Table of Contents artwork